AU/ACSC/054/1999-04

AIR COMMAND AND STAFF COLLEGE

AIR UNIVERSITY

# SYMMETRIC CONVOLUTION

# USING UNITARY TRANSFORM MATRICES:

## A NEW APPROACH TO IMAGE RECONSTRUCTION

by

Thomas M. Foltz, Major, USAF

A Research Report Submitted to the Faculty

In Partial Fulfillment of the Graduation Requirements

Advisor: Major Courtney D. Holmberg

Maxwell Air Force Base, Alabama

April 1999

## Disclaimer

# *Contents*

## *Illustrations*

*Page*

## *Acknowledgments*

I wish to thank my *advisor*, Major Court Holmberg, for allowing me to pursue this line of research, for getting me started down its path, and for seeing it through to completion. I also wish to thank Dr. Byron Welsh of Mission Research Corporation, Dayton, Ohio, who also serves as an adjunct professor of electrical engineering at the Air Force Institute of Technology, Wright-Patterson AFB, Ohio; Dr. Bill Martel, Director of the Center for Strategy and Technology, Air War College, Maxwell AFB, Alabama; and Capt Steve Ford of Air Force Research Lab, Kirtland AFB, New Mexico, for their genuine interest and sincere support of this research project.

I also wish to thank my wife, Julie, and sons, Jim and Sam. Even though they are used to the large time sink brought on by a research project, none of them even winced when they found out last August that I would be tackling this one. I know they did not enjoy the hours spent away from activities with them, and I admire their patience and perseverance.

## *Abstract*

The Air Force images space-borne objects from the ground with optical systems that suffer from the effects of atmospheric turbulence. Many image processing techniques exist to alleviate these effects, but they are computationally complex and require large amounts of processing time. A faster image processing system would greatly improve images of objects observed through the turbulent atmosphere and help national strategists glean higher quality intelligence on other nations' space platforms. One promising mathematical method to decrease the computational complexity of image processing algorithms involves symmetric convolution. Symmetric convolution is a recently discovered property of trigonometric transforms that allows the convolution of sequences to be calculated through point multiplication in the trigonometric transform domain. This method holds distinct advantages over existing matrix techniques. The versions of the transform matrices for symmetric convolution are similar but not exactly equal to standard unitary versions of trigonometric transforms. This paper demonstrates relationships between the two types of transform matrices, and then uses the new relationships to derive forms of the symmetric convolution-multiplication property based on unitary rather than convolutional forms of the transform matrices. It further describes how image processing algorithms based on unitary transforms can be included in future-generation optical surveillance systems.

## Chapter 1

# Introduction

The Air Force has a need to image space-borne objects from the ground.[1] Air Force analysts can use these images to discern details about the capabilities of an adversary's satellite systems. National level strategists can use images of space-borne platforms to verify compliance with existing treaties on nonproliferation of space-based weapons. When trained on our own satellites, ground-based imaging systems can also provide satellite maintainers information about the health and well-being of our own systems. Additionally, the Air Force has recently entered a joint venture with the Jet Propulsion Laboratory to detect and classify the orbits of asteroids that may approach the orbital plane of the earth.[2]

One factor severely limiting the performance of ground-based optical systems is atmospheric turbulence.[3] The constant motion of different layers of the atmosphere causes the indices of refraction within those layers to change, which in turn causes scattering of the light captured within the aperture of a telescope on the ground. This scattering causes images to appear much more blurred than if the turbulent effects of the atmosphere were not present. The objective of this research is to demonstrate new techniques that the Air Force can use to improve its methods of collecting information on space-borne objects.

The process of restoring a degraded image is referred to as image reconstruction.[4] A variety of mathematically complex convolutional techniques exist to perform image reconstruction via filtering. Symmetric convolution is a recently discovered property[5] of discrete trigonometric transforms that allows for the filtering of images to be calculated through point multiplication in the trigonometric transform domain at a tremendous savings in computational complexity over computing the convolution sum directly. Symmetric convolution has already been demonstrated as a method to mathematically enhance existing image reconstruction techniques.[6] The existing form of the symmetric convolution-multiplication property is, however, somewhat limited in that the versions of the transform matrices for symmetric convolution are similar but not exactly equal to the standard unitary versions of trigonometric transforms.

This paper demonstrates a relationship between the two types of trigonometric transform matrices—convolutional and unitary. It then proves how the new relationships can be used to derive forms of the symmetric convolution-multiplication property based on unitary rather than convolutional forms of the transform matrices. The paper further describes how image processing algorithms based on unitary transforms can be included in future-generation optical surveillance systems to improve existing image reconstruction techniques used by the Air Force.

The objectives of this research are directly related to the Air Force's core competency of information superiority. Air Force Doctrine Document 1 (AFDD-1) defines information superiority as "the ability to collect, control, exploit, and defend information while denying an adversary the ability to do the same."[7] The results of this research will help the Air Force in its efforts to collect information by improving techniques to mitigate the effects of atmospheric turbulence. The end results of these efforts will enhance the Air Force's function as "the major operator of sophisticated air- and space-based intelligence, surveillance, and reconnaissance systems and [as] the Service most able to quickly respond to the information they provide."[8]

The remainder of this paper is organized to provide the reader with enough information to understand the problem as well as grasp the benefits offered by symmetric convolution. Chapter 2 contains general background information on how the Air Force currently images space-borne objects from the ground. Chapter 3 provides technical background information on image reconstruction, symmetric convolution and the discrete trigonometric transforms, and on how symmetric convolution can be used to perform image reconstruction. Chapter 4 derives the relationship between convolutional and unitary discrete trigonometric transforms by first demonstrating that diagonal matrices exist which relate the two versions, and then proving that new vector-matrix forms of the symmetric convolution-multiplication property exist that are based on unitary rather than convolutional discrete trigonometric transforms. Chapter 5 gives a proposal for how image processing algorithms based on the new unitary versions of the symmetric convolution-multiplication property can be included in future-generation optical surveillance systems with faster processing times and improved image quality. Chapter 6 summarizes the findings and outlines directions for future research.

## Notes

[1] Capt Stephen D. Ford, "Linear Reconstruction of Non-Stationary Image Ensembles Incorporating Blur and Noise Models," Ph.D. Dissertation, AFIT/DS/ENG/98-02. Air Force Institute of Technology (AETC), Wright-Patterson AFB, Ohio, March 1998, 1–5.

[2] "Air Force Research Laboratory's Mission on Maui," *AMOS WWW Homepage,* 29 April 1998, n.p.; on-line, Internet, available from http://ulua.mhpcc.af.mil.

[3] Michael C. Roggemann and Byron M. Welsh, *Imaging Through Turbulence*. (Boca Raton, Fla.: CRC Press, 1996), 1–3.

[4] Ibid., 158–166.

[5] Stephen A. Martucci, "Symmetric Convolution and the Discrete Sine and Cosine Transforms," *IEEE Transactions on Signal Processing* 42, no. 5 (May 1994): 1038–1046.

[6] See for example:

Maj Thomas M. Foltz, "Trigonometric Transforms for Image Reconstruction," Ph.D. Dissertation, AFIT/DS/ENG/98-04. Air Force Institute of Technology (AETC), Wright-Patterson AFB, Ohio, June 1998, 1–122.

Foltz and B.M. Welsh, "A Scalar Wiener Filter Based on Discrete Trigonometric Transforms and Symmetric Convolution," in *Proceedings of the SPIE, Vol. 3433, Propagation and Imaging through the Atmosphere II*, San Diego, Calif., (July 1998): 285–295.

and

Foltz and Welsh, "Image Reconstruction Using Symmetric Convolution and Discrete Trigonometric Transforms," *Journal of the Optical Society of America A* 15, no. 11 (November 1998): 2827–2840.

[7] Air Force Doctrine Document (AFDD) 1. *Air Force Basic Doctrine,* September 1997, 31–32.

[8] Ibid., 31.

# Chapter 2

## General Background

This chapter provides general background information on existing Air Force methods for imaging space-borne objects from the ground. In particular, it discusses Air Force efforts to use adaptive optics systems and laser beacons to reduce the effects of atmospheric turbulence as well as describing post-processing techniques to reconstruct images.

As was stated earlier, the effects of turbulence on light passing through the atmosphere create this imaging problem. To illustrate the severity of the problem, consider that "at [one of] the best observing sights—in Hawaii…—where there are telescopes of up to 10 meters in diameter, turbulence still limits the resolution to the equivalent of that achieved by a telescope only 10 cm in diameter [without turbulence]."[1] By comparison, the Hubble space telescope, which obviously does not suffer from the degrading effects of atmospheric turbulence, is only 2 meters in diameter but cost a great deal to launch into orbit. Bigger telescopes on the ground allow more light to pass through their apertures—a necessary feature to image dim objects.

One technique to reduce the effects of atmospheric turbulence is through the use of *adaptive optics*. Adaptive optics systems use a wavefront sensor to measure the scattering from a bright object in the vicinity of the object to be imaged. The system sends control signals to a series of actuators that physically adjust the contour of a telescope's deformable mirror to correct for the perturbations caused by the atmosphere.[2] The system must correct itself about 100 times each second to keep up with the rate of changes in the atmosphere.

In a recent *Scientific American* article,[3] John Hardy, a pioneer of adaptive optics research who recently retired from Litton Itek Optical Systems, describes the history of the first operational adaptive optics system. He states that the project began in the 1970s as a Defense Advanced Research Projects Agency (now ARPA) effort to better identify the high numbers of military satellites the Soviet Union was launching at the time. He claims that after testing a prototype system with 21 actuators in December 1973, ARPA next installed an adaptive optics system employing 168 actuators on a 1.6 meter telescope atop Mount Haleakala in Maui, Hawaii in 1980. The system was first tested in the spring of 1982 with impressive results, especially for images of binary star pairs.[4]

Today Mount Haleakala is home to the Air Force Research Laboratory's (AFRL's) research and development efforts on the Maui Space Surveillance System (MSSS) at the Maui Space Surveillance Complex (MSSC), formerly the Air Force Maui Optical Station (AMOS).[5] The MSSS instruments all suffer from the effects of atmospheric turbulence despite the fact that the ten thousand foot elevation of the complex, the dry climate, and freedom from background light pollution all allow unsurpassed detection of satellites, missiles, man-made orbital debris and astronomical objects.[6]

In a recent *Physics Today* article,[7] Laird Thompson, professor of astronomy at the University of Illinois at Urbana-Champaign, reports on recent advances in adaptive optics including Air Force efforts at the Starfire Optical Range (SOR) in New Mexico. He also provides background information on a technique that provides an alternative to the requirement of an adaptive optics system to have a bright object in the vicinity of the object being imaged. This technique uses a laser beacon or guide "star" which is a beam of laser light shot into the night sky that scatters off molecules in the stratosphere at altitudes of 10–20 km. The scattered light creates the same effect as a bright natural star on the order of 0.1 magnitude. Previous adaptive optics systems required a natural star in the vicinity of the object to be imaged to measure the turbulence with a wavefront sensor. Thompson further discusses research efforts to use experimental lasers to scatter light off sodium atoms in the mesosphere at altitudes of 95 km. The higher altitude would decrease the amount of anisoplanatism or angular error in the laser guide star reference. Thompson describes the explosive growth of adaptive optics and laser guide star research in the early part of this decade:

> What astronomers thought in the late 1980s would be an evolutionary drift toward adaptive optics turned into a veritable revolution in the spring of 1991, when US military researchers stepped forward to announce that they too had been investing in both adaptive optics and laser-guide star research.[8]

Thompson gives three reasons he suspects led to the military's decision to release information on its efforts at adaptive optics and laser guide star research. He offers that European researchers had prototyped an infrared adaptive optics system, his own team at the University of Illinois had published the results of successful experiments using laser guide stars, and these results coincided with the end of the cold war. Figure 1 from the AMOS webpage[9] shows a laser guide star in action on the top of Mount Haleakala. The system in use is known as SWAT (for short wavelength adaptive technique).[10] According-

## Notes

[1] Clive Standley, “Adaptive Optics Compensates for Atmospheric Distortion,” *Laser Focus World* 34, no. 6 (June 1998): 90.

[2] Michael C. Roggemann and Byron M. Welsh, *Imaging Through Turbulence*. (Boca Raton, Fla.: CRC Press, 1996), 178–182.

[3] John W. Hardy, “Adaptive Optics—Technology developed during the cold war is giving new capabilities to ground-based astronomical telescopes,” *Scientific American* 270, no. 6 (June 1994): 60–65.

[4] Ibid., 63.

[5] “Air Force Research Laboratory’s Mission on Maui,” *AMOS WWW Homepage*, 29 April 1998, n.p.; on-line, Internet, available from http://ulua.mhpcc.af.mil.

[6] Ibid.

[7] Laird A. Thompson, “Adaptive Optics in Astronomy,” *Physics Today* 47, no. 12 (December 1994): 24–31.

[8] Ibid., 27.

[9] *AMOS WWW Homepage.*

[10] Hardy, 65.

**Figure 1. AMOS Observatory**

ing to Hardy,[1] this system was proposed by Robert Fugate of Phillips Laboratory and developed by researchers at M.I.T. Lincoln Laboratory.

In addition to adaptive optics with natural or artificial guide stars, another method of performing image reconstruction is to use image processing.[2] Similar to adaptive optics techniques, some image processing systems can measure the effects of atmospheric perturbations, and then use a computer to correct for the effects of the distortion. Such systems are often called post-processing systems since they perform their calculations "after the fact" instead of "on the fly" as for adaptive optics systems. Other image processing techniques require no *a priori* knowledge of the turbulence. They do not require a wavefront sensor to measure the turbulence, and instead apply nonlinear iterative algorithms to deduce both a turbulence-compensated image and a mathematical model of the turbulence that caused the degradation in the original image.[3] Still other image processing techniques are linear in nature, *i.e.* they can correct an image in a single direct iteration, but they require knowledge of at least the statistics of the turbulence degrading the image.[4] These techniques require fewer computations than iterative techniques, but they suffer from poorer performance than either wavefront sensor processing, iterative processing, or adaptive optics.

The tradeoff between computational complexity vs. higher performance image reconstruction algorithms is a problem of interest to the developers of the next generation of Air Force optical systems. The computational speed of adaptive optics systems limits the number of frames or snapshots that the system can obtain each second. The faster a processor can perform its calculations on turbulence measurements, the faster the system can provide updates on changing atmospheric conditions. Similarly, the faster a post-processing technique can generate a turbulence-compensated image, the faster the image can be sent to analysts and the quicker the computer can be turned over to perform calculations on other images.

The mathematical relationships derived in later chapters of this paper can help improve the performance of Air Force systems using adaptive optics by increasing the speed of transform domain calculations used to correct for turbulence. The results of this research stand to pose an even greater benefit to linear systems that perform image post-processing, because they can speed up each calculation within an iterative algorithm. These improvements also benefit linear direct-calculation systems, not only because they perform calculations quicker, but also because the trigonometric transforms upon which they are based have performance advantages over other more conventional transforms.[5]

This chapter has provided a brief introduction to how the Air Force images space-borne objects from the ground. Prior to proceeding with the derivations contained in later chapters, it is first necessary to present some mathematical background information in the next chapter.

**Notes**

[1] Ibid.

[2] Roggemann and Welsh, Chapter 4, 123–168.

[3] Both

G.R. Ayers and J.C. Dainty, "Iterative Blind Deconvolution Method and its Applications," *Optics Letters* 13, no. 7 (July 1988): 547–549.

and

B.L.K. Davey, R.G. Lane, and R.H.T. Bates, "Blind Deconvolution of Noisy Complex-Valued Image," *Optics Communications* 69, no. 5,6 (January 15, 1989): 353–356.

describe iterative techniques to solve this problem known as *blind deconvolution.*

[4] For early work on least-squares linear filtering, see

Carl W. Helstrom, "Image Restoration by the Method of Least Squares," *Journal of the Optical Society of America* 57, no. 3 (March 1967): 297–303.

## Notes

David Slepian, "Linear Least-Squares Filtering of Distorted Images," *Journal of the Optical Society of America* 57, no. 7 (July 1967): 918–922.

and

William K. Pratt, "Generalized Wiener Filter Computation Techniques," *IEEE Transactions on Computers* C-21, no. 7 (July 1972): 636–641.

Excellent summaries of these types of techniques appear in

Anil K. Jain, *Fundamentals of Digital Image Processing*. (Englewood Cliffs, N.J.: Prentice-Hall, 1989), Chapter 8, 267–341.

and

Rafael C. Gonzalez and Richard E. Woods, *Digital Image Processing*. (Reading, Mass.: Addison-Wesley, 1992), Chapter 5, 253–305.

[5] Jain, 150–155.

# Chapter 3

# Technical Background

This chapter lays the technical foundation upon which the derivations in the following chapter are based by establishing a consistent mathematical notation and presenting the results of previous research related to symmetric convolution and its applications for image reconstruction. The following sections supply theoretical information on the basic image reconstruction problem, symmetric convolution and the discrete trigonometric transforms (DTTs), and a discussion on how the symmetric convolution-multiplication property can be applied to improve linear image reconstruction techniques.

## Image Reconstruction

Image reconstruction is the process of restoring degraded images.[1] An imaging system typically measures a blurred, noisy image of an object. In the problem of imaging space-borne objects from the ground, the blurring is caused by the turbulent atmosphere which has a severe degrading effect on the quality of images[2] and random noise that is always present in image detection systems.[3] The system must then apply image reconstruction techniques to recover an estimate of the object from its blurred, noisy version. One technique used to perform this task is linear filtering.

To help illustrate how a filter can recover an estimate of an object from its distorted, noisy version, consider the imaging scenario in Figure 2. In the figure, the two-dimen-

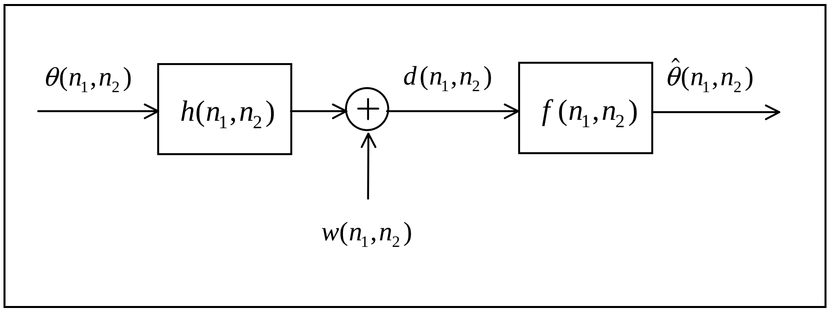


**Figure 2. Imaging Scenario**

sional sequence $\theta(n_1,n_2)$ represents the original object, where the indices $n_1$ and $n_2$ correspond to an ordering of the pixels of the image. The two-dimensional sequence $h(n_1,n_2)$ represents the point spread function of the system blurring the object. Optical scientists and engineers refer to the two-dimensional impulse response of the degrading system as its point spread function. The name arises from the blurring or spreading of individual points comprising the object.[4] The scenario adds noise represented by the sequence $w(n_1,n_2)$ to produce the received data sequence $d(n_1,n_2) = h(n_1,n_2) * \theta(n_1,n_2) + w(n_1,n_2)$. The asterisk, *, denotes the convolution operation, which can also be expressed as[5]

$$h(n_1,n_2) * \theta(n_1,n_2) = \sum_{m_1=-\infty}^{\infty} \sum_{m_2=-\infty}^{\infty} \theta(m_1,m_2) h(m_1-n_1, m_2-n_2). \tag{1}$$

The recovery filter in the scenario has a two-dimensional impulse response, $f(n_1,n_2)$, so that the estimate of the object is $\hat{\theta}(n_1,n_2) = f(n_1,n_2) * d(n_1,n_2)$. The goal of image reconstruction with a linear filter is to find the impulse response of the recovery filter, $f(n_1,n_2)$, which produces the best possible estimate $\hat{\theta}(n_1,n_2)$.

If the sequences in Eq. (1) are spatially limited to $N_1 \times N_2$ pixels, then an easier way to calculate the convolution sum is to first convert each sequence into its discrete Fourier transform (DFT) representation, $H(k_1,k_2)$ and $\Theta(k_1,k_2)$, where[6]

$$H(k_1,k_2) = \sum_{n_1=0}^{N_1-1} \sum_{n_2=0}^{N_2-1} h(n_1,n_2) \exp\left\{-j\frac{2\pi n_1 k_1}{N_1}\right\} \exp\left\{-j\frac{2\pi n_2 k_2}{N_2}\right\},$$

and

$$\Theta(k_1,k_2) = \sum_{n_1=0}^{N_1-1} \sum_{n_2=0}^{N_2-1} \theta(n_1,n_2) \exp\left\{-j\frac{2\pi n_1 k_1}{N_1}\right\} \exp\left\{-j\frac{2\pi n_2 k_2}{N_2}\right\}. \tag{2}$$

A well-known property of DFTs states that convolution in the spatial domain is equivalent to point-wise multiplication in the transform domain of the DFTs.[7] It thus requires fewer calculations to perform the two DFTs in Eq. (2), compute the product $H(k_1,k_2) \times \Theta(k_1,k_2)$, and then perform an inverse DFT to yield the same result as Eq. (1). Hunt[8] has shown the summations in Eqs. (1) and (2) can be expressed as a vector-matrix multiplication, and that matrices representing the DFT operation can diagonalize a matrix representing the convolution operation.

Another family of transforms that are similar to the DFT and useful for image processing are the discrete cosine and sine transforms (DCTs and DSTs).[9] Until recently no convolution-multiplication property existed for the discrete trigonometric transforms (DTTs), so their application to image reconstruction filtering is a relatively new concept.

## Symmetric Convolution and the Discrete Trigonometric Transforms

The discrete cosine transform was first introduced in 1974.[10] Since then it has been expanded into an entire family of trigonometric transforms[11] consisting of sixteen DTTs which are even and odd-length versions of the DSTs and DCTs. Another characteristic of the family of DTTs is that each transform is one of four types (I–IV) that impose half-sample shifts in the input or output indices of the sine and cosine transforms. A type-I trigonometric transform imposes no shift to either the input or the output sequence indices. A type-II transform imposes a half-sample shift to just the input index. A type-III transform imposes a half-sample shift to just the output index. A type-IV transform imposes a half-sample shift to both the input and the output indices. The fact that these four transforms require either no shift or a half-sample shift is related to the idea of the point of symmetry in the symmetric extension of a finite sequence. The point of symmetry can be either an end point of the sequence or a point which lies one-half sample beyond the end point of the sequence.

There are four ways to symmetrically extend a finite sequence about a single point of symmetry. These are *whole-sample symmetry* (WS), *whole-sample antisymmetry* (WA), *half-sample symmetry* (HS), and *half-sample antisymmetry* (HA). An example of each appears in Figure 3. Note that the point of symmetry for the WS sequence is the end point in the finite sequence before extension, and the point of symmetry for the WA sequ-

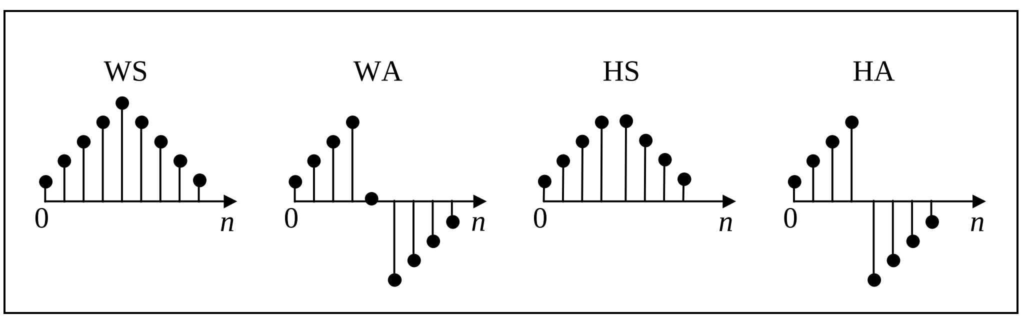


**Figure 3. Four Ways to Symmetrically Extend a Finite Sequence**[12]

ence is a zero that must appear after the end point before extension. The points of symmetry for both the HS and HA sequences lie one-half sample beyond the end points in each finite sequence before extension.

There are 16 *symmetric periodic sequences* (SPS's) which result from symmetrically extending a finite sequence to the left using one of the four ways and to the right using possibly a different way. A convention for naming each of the 16 SPS's is to label first the left symmetric extension and then the right symmetric extension. For example, a WSHA sequence would exhibit whole-sample symmetry to the left and half-sample antisymmetry to the right. A one-to-one correspondence exists between the sixteen types of SPS's and the sixteen DTTs.[13]

Martucci[14] has recently developed a convolution-multiplication property for the family of DTTs based upon the underlying symmetry of each DTT. He defines *symmetric convolution* as the form of convolution for DTTs. The symmetric convolution-multiplication property states that an inverse trigonometric transform of the product of the trigonometric transforms of two sequences yields the same result as the symmetric convolution of the two sequences.[15] The symmetric convolution-multiplication property exists for forty different combinations of the sixteen transforms in the DTT family based on the underlying symmetric periodicities of the different DTTs.

In the derivation of his symmetric convolution-multiplication property, Martucci[16] slightly redefines each of the DTTs into what he refers to as their *convolutional versions*. The modifications are necessary to relate each DTT to the more generalized DFT of Bongiovanni *et al.*[17] upon which Martucci's derivation is based. Definitions for each of the sixteen convolutional versions and for each of the more traditional versions of the DTTs appear in Appendix A. Note that the traditional versions of the DTTs are all represented by unitary matrices. An $N \times N$ unitary matrix, $\boldsymbol{U}$, has the property that $\boldsymbol{U}^T = \boldsymbol{U}^{-1}$, or equivalently $\boldsymbol{U}\boldsymbol{U}^T = \boldsymbol{I}_N$, where the superscript '*T*' indicates the transpose of a matrix and the matrix $\boldsymbol{I}_N$ is an $N \times N$ identity matrix.

Martucci defines forty cases of the symmetric convolution-multiplication property based on the sixteen convolutional versions of the DTTs listed in Appendix A. Just as Hunt[18] presented a vector-matrix relationship for the convolution-multiplication property of the DFT, recent research[19] has revealed diagonal forms of the symmetric convolution-multiplication property for each of the forty cases of symmetric convolution. Sánchez *et al.* have previously demonstrated the existence of diagonal forms of the convolutional versions of the DTTs,[20] but their results reveal diagonalizing forms for only sixteen of the forty cases of symmetric convolution—one case of symmetric convolution for each of the sixteen transforms. The vector-matrix forms of all forty cases appear in Appendix B. The advantages to a vector-matrix form of each case include compactness of notation and the fact that the property extends more easily to asymmetric multidimensional sequences which is a necessary condition to apply the property to image reconstruction.

## Image Reconstruction Using Symmetric Convolution

This section demonstrates results for the two-dimensional impulse response of a linear image reconstruction filter that is optimum in the mean-square sense for reconstructing images degraded by a known blurring function in the presence of additive noise.[21] Such filters are commonly referred to as Wiener filters after the pioneering work of Norbert Wiener in the 1940s.[22] Both Helstrom[23] and Slepian[24] have applied Wiener filters to the least-squares image reconstruction problem.

Pratt[25] has outlined the vector-matrix form of the image reconstruction problem which is to find the filter represented as a matrix, $\boldsymbol{F}$, that produces the vector estimate $\hat{\boldsymbol{\theta}} = \boldsymbol{F}\boldsymbol{d}$ arising from linearly corrupted data in noise from the relation $\boldsymbol{d} = \boldsymbol{H}\boldsymbol{\theta} + \boldsymbol{w}$ depicted graphically in Figure 2. The estimate, $\hat{\boldsymbol{\theta}}$, should be the estimate which minimizes the mean-square error between the estimate and the original object vector, $\boldsymbol{\theta}$. The solution for the filter, $\boldsymbol{F}$, that produces the minimum mean-square error estimate, $\hat{\boldsymbol{\theta}}$, is well documented in statistical signal processing texts[26] as

$$\boldsymbol{F} = \boldsymbol{R}_{\theta\theta}\boldsymbol{H}^T\left[\boldsymbol{H}\boldsymbol{R}_{\theta\theta}\boldsymbol{H}^T + \boldsymbol{R}_{ww}\right]^{-1}, \tag{3}$$

where $\boldsymbol{R}_{\theta\theta}$ and $\boldsymbol{R}_{ww}$ are correlation matrices for the object and noise respectively.

The trigonometric transform domain realization of Eq. (3) then becomes

$$\mathcal{F}_{ss}(k_1,k_2) = \frac{\mathcal{H}_{ss}(k_1,k_2)}{\mathcal{H}_{ss}^2(k_1,k_2) + \dfrac{\overline{\mathcal{W}_{ss}^2(k_1,k_2)}}{\Theta_{ss}^2(k_1,k_2)}}, \tag{4}$$

where the script letters denote that the quantities lie in the trigonometric transform domain and the subscripts '*ss*' indicate the relation holds only for functions possessing whole-sample symmetry in both spatial dimensions. Note that Eq. (4) is a scalar and not a matrix relation. The scalar nature of Eq. (4) arises because the vector-matrix form of the symmetric convolution-multiplication property produces a diagonal matrix in the transform domain, and also because the type-II DCT produces a nearly diagonal correlation matrix in the transform domain for an image with highly correlated pixels.[27] This fact is significant because scalar relations require far fewer calculations to implement than matrix relations.

One limitation of Eq. (4) is that it is only valid for the convolutional versions of the DTTs. The unitary versions of the DTTs are more common and hardware exists to incorporate fast implementations of the transforms. The next step in this process is to derive forms of the symmetric convolution-multiplication property based on unitary rather than convolutional versions of the DTTs. This derivation will be the primary focus of the next chapter.

**Notes**

[1] Anil K. Jain, *Fundamentals of Digital Image Processing*. (Englewood Cliffs, N.J.: Prentice-Hall, 1989), 267–268.

[2] Michael C. Roggemann and Byron M. Welsh, *Imaging Through Turbulence*. (Boca Raton, Fla.: CRC Press, 1996), Chapter 3, 57–122.

[3] Joseph W. Goodman, *Statistical Optics*. (New York: John Wiley and Sons, 1985), 60.

[4] Goodman, *Fourier Optics*. (New York: McGraw-Hill, 1968), 18–21.

[5] Alan V. Oppenheim and Ronald W. Schafer, *Digital Signal Processing*. (Englewood Cliffs, N.J.: Prentice-Hall, 1975), 32.

[6] Ibid., 117.

[7] Ibid., 105–109.

[8] B.R. Hunt, "A Matrix Theory Proof of the Discrete Convolution Theorem," *IEEE Transactions on Audio and Electroacoustics* AU-19, no. 4 (December 1971): 285–288.

and

Hunt, "The Application of Constrained Least Squares Estimation to Image Restoration by Digital Computer," *IEEE Transactions on Computers* C-22, no. 9 (September 1973): 805–812

[9] Jain, Chapter 8, 150–155.

[10] N. Ahmed, T. Natarajan, and K.R. Rao, "Discrete Cosine Transform," *IEEE Transactions on Computers* C-23, no. 1 (January 1974): 90–93.

[11] Original publications of the different members of the family of DTTs include

H.B. Kekre and J.K. Solanki, "Comparative Performance of Various Trigonometric Unitary Transforms for Image Coding," *International Journal of Electronics* 44, no. 3 (March 1978): 305–315.

William K. Pratt, *Digital Image Processing*. (New York: John Wiley and Sons, 1978), 242–250.

and

**Notes**

Jain, “A Sinusoidal Family of Unitary Transforms,” *IEEE Transactions on Pattern Analysis and Machine Intelligence* PAMI-1, no. 4 (October 1979): 356–365.

with a complete list appearing in

Zhongde Wang and Hunt, “The Discrete W Transform,” *Applied Mathematics and Computation* 16, no. 1 (January 1985): 33–35.

[12] Stephen A. Martucci, “Symmetric Convolution and the Discrete Sine and Cosine Transforms,” *IEEE Transactions on Signal Processing* 42, no. 5 (May 1994): 1041.

[13] Ibid., 1041–1043.

[14] Ibid., 1038–1051.

[15] Ibid.

[16] Ibid., 1040, 1050.

[17] Giancarlo Bongiovanni, Paolo Corsini, and Graziano Frosini, “One Dimensional and Two-Dimensional Generalized Discrete Fourier Transforms,” *IEEE Transactions on Acoustics, Speech, and Signal Processing* ASSP-24, no. 1 (February 1976): 97–99.

[18] Hunt, 1971, and Hunt, 1973.

[19] See for example:

Maj Thomas M. Foltz, “Trigonometric Transforms for Image Reconstruction,” Ph.D. Dissertation, AFIT/DS/ENG/98-04. Air Force Institute of Technology (AETC), Wright-Patterson AFB, Ohio, June 1998, 1–122.

Foltz and B.M. Welsh, “A Scalar Wiener Filter Based on Discrete Trigonometric Transforms and Symmetric Convolution,” in *Proceedings of the SPIE, Vol. 3460, Applications of Digital Image Processing XXI*, San Diego, Calif., (July 1998): 214–225.

and

Foltz and Welsh, “Symmetric Convolution of Asymmetric Multidimensional Sequences Using Discrete Trigonometric Transforms,” to appear in *IEEE Transactions on Image Processing* 8, no.5 (May 1999).

[20] Victoria Sánchez, Pedro García, Antonio M. Peinado, José C. Segura, and Antonio J. Rubio, “Diagonalizing Properties of the Discrete Cosine Transforms,” *IEEE Transactions on Signal Processing* 43, no. 11 (November 1995): 2631–2641.

and

Sánchez, Peinado, Segura, García, and Rubio, “Generating Matrices for the Discrete Sine Transforms,” *IEEE Transactions on Signal Processing* 44, no. 10 (October 1996): 2644–2646.

[21] Foltz and Welsh, “A Scalar Wiener Filter Based on Discrete Trigonometric Transforms and Symmetric Convolution,” in *Proceedings of the SPIE, Vol. 3433, Propagation and Imaging through the Atmosphere II*, San Diego, Calif., (July 1998): 285–295.

and

Foltz and Welsh, “Image Reconstruction Using Symmetric Convolution and Discrete Trigonometric Transforms,” *Journal of the Optical Society of America A* 15, no. 11 (November 1998): 2827–2840.

[22] Norbert Wiener, *Extrapolation, Interpolation, and Smoothing of Stationary Time Series*. (New York: John Wiley and Sons, 1949).

[23] Carl W. Helstrom, “Image Restoration by the Method of Least Squares,” *Journal of the Optical Society of America* 57, no. 3 (March 1967): 297–303.

## Notes

[24] David Slepian, “Linear Least-Squares Filtering of Distorted Images,” *Journal of the Optical Society of America* 57, no. 7 (July 1967): 918–922.

[25] Pratt, “Generalized Wiener Filter Computation Techniques,” *IEEE Transactions on Computers* C-21, no. 7 (July 1972): 636–641.

[26] See for example:

Louis L. Scharf, *Statistical Signal Processing: Detection, Estimation, and Time Series Analysis*. (Reading, Mass.: Addison-Wesley, 1991), Chapter 9, 359–422.

Charles W. Therrien, *Discrete Random Signals and Statistical Signal Processing*. (Englewood Cliffs, N.J.: Prentice-Hall, 1992), Chapter 7, 337–408.

or

Steven M. Kay, *Fundamentals of Statistical Signal Processing*. (Englewood Cliffs, N.J.: Prentice-Hall, 1993), Chapter 12, 379–418.

[27] Jain, 1989, 150–155.

# Chapter 4

# Relationship between Convolutional and Unitary Transforms

This chapter presents the mathematical relationship between the convolutional versions of the discrete trigonometric transforms (DTTs) and the more common unitary versions of the DTTs. For nine out of the sixteen transforms in the DTT family, the relationship is diagonal. The diagonal matrices which relate the two versions of the DTTs then allow the vector-matrix form of the symmetric convolution property to be cast in terms of unitary rather than convolutional transforms.[1]

## Diagonal Matrices Relating the Two Versions

This section demonstrates the relationships between each of the sixteen convolutional DTTs and their unitary counterparts. Consider the following matrix relationships between convolutional and unitary DTT matrices:

$$\begin{array}{llll} \boldsymbol{C}_{1e} = \boldsymbol{A}_1 \boldsymbol{C}_{\mathrm{I}e} & \boldsymbol{C}_{2e} = \boldsymbol{A}_2 \boldsymbol{C}_{\mathrm{II}e} & \boldsymbol{C}_{3e} = \boldsymbol{A}_3 \boldsymbol{C}_{\mathrm{III}e} & \boldsymbol{C}_{4e} = \boldsymbol{A}_4 \boldsymbol{C}_{\mathrm{IV}e} \\ \boldsymbol{S}_{1e} = \boldsymbol{A}_5 \boldsymbol{S}_{\mathrm{I}e} & \boldsymbol{S}_{2e} = \boldsymbol{A}_6 \boldsymbol{S}_{\mathrm{II}e} & \boldsymbol{S}_{3e} = \boldsymbol{A}_7 \boldsymbol{S}_{\mathrm{III}e} & \boldsymbol{S}_{4e} = \boldsymbol{A}_8 \boldsymbol{S}_{\mathrm{IV}e} \\ \boldsymbol{C}_{1o} = \boldsymbol{A}_9 \boldsymbol{C}_{\mathrm{I}o} & \boldsymbol{C}_{2o} = \boldsymbol{A}_{10} \boldsymbol{C}_{\mathrm{II}o} & \boldsymbol{C}_{3o} = \boldsymbol{A}_{11} \boldsymbol{C}_{\mathrm{III}o} & \boldsymbol{C}_{4o} = \boldsymbol{A}_{12} \boldsymbol{C}_{\mathrm{IV}o} \\ \boldsymbol{S}_{1o} = \boldsymbol{A}_{13} \boldsymbol{S}_{\mathrm{I}o} & \boldsymbol{S}_{2o} = \boldsymbol{A}_{14} \boldsymbol{S}_{\mathrm{II}o} & \boldsymbol{S}_{3o} = \boldsymbol{A}_{15} \boldsymbol{S}_{\mathrm{III}o} & \boldsymbol{S}_{4o} = \boldsymbol{A}_{16} \boldsymbol{S}_{\mathrm{IV}o}, \end{array} \tag{5}$$

where the matrices denoted by $\boldsymbol{C}$ and $\boldsymbol{S}$ represent discrete cosine and sine transform (DCT and DST) matrices respectively. The numeric subscripts '1–4' represent DTT transform types I–IV for the convolutional versions of DTT matrices, and the Roman numeral subscripts 'I–IV' represent DTT transform types I–IV for the unitary versions of

DTT matrices. The subscripts *'e'* and *'o'* denote even and odd length versions of the DTT matrices. Complete definitions for the convolutional and unitary versions appear in Appendix A. The matrices $\boldsymbol{A}_1 - \boldsymbol{A}_{16}$ relate the two versions for each of the sixteen DTTs.

To express symmetric convolution in terms of unitary transforms, only those matrices from $\boldsymbol{A}_1 - \boldsymbol{A}_{16}$ that are diagonal are useful for subsequent derivations because the matrix form of symmetric convolution results in diagonal matrices in the trigonometric transform domain. It is straightforward to show by counterexample that the matrices $\boldsymbol{A}_1$, $\boldsymbol{A}_3$, $\boldsymbol{A}_7$, $\boldsymbol{A}_9$, $\boldsymbol{A}_{10}$, $\boldsymbol{A}_{11}$, and $\boldsymbol{A}_{16}$ are not, in general, diagonal. To show that the matrix $\boldsymbol{A}_2$ is, in general, diagonal, consider that the matrix $\boldsymbol{C}_{\mathrm{II}e}$ is unitary, *i.e.* $\boldsymbol{C}_{\mathrm{II}e}\boldsymbol{C}_{\mathrm{II}e}^T = \boldsymbol{I}_N$, an $N \times N$ identity matrix, which allows the matrix $\boldsymbol{A}_2$ to be written as $\boldsymbol{A}_2 = \boldsymbol{C}_{2e}\boldsymbol{C}_{\mathrm{II}e}^T$. Repeating the definitions for the $m-n$th elements of the $N \times N$ type-II even-length DCT matrices from Appendix A, yields

$$[\boldsymbol{C}_{2e}]_{mn} = 2\cos\left(\frac{\pi m(n+\tfrac{1}{2})}{N}\right), \tag{6}$$

and

$$[\boldsymbol{C}_{\mathrm{II}e}]_{mn} = \sqrt{\frac{2}{N}k_m}\cos\left(\frac{\pi m(n+\tfrac{1}{2})}{N}\right), \tag{7}$$

for $m, n = 0, 1, \ldots, N-1$. The constant, $k_m$, in Eq. (7) differs from Wang and Hunt's definition,[2] so that

$$k_m = \begin{cases} \tfrac{1}{2}, & m = 0, N \\ 1, & \text{otherwise,} \end{cases} \tag{8}$$

which follows the convention for Martucci's convolutional versions.[3] Equation (7) yields a unitary matrix equivalent to Wang and Hunt's definition[4] for any even *N*. It follows from Eqs. (6) and (7) that

$$[\boldsymbol{C}_{2e}]_{mn} = \sqrt{\frac{2N}{k_m}}[\boldsymbol{C}_{\mathrm{II}e}]_{mn}. \tag{9}$$

The $m-n$th element of the product $\boldsymbol{A}_2 = \boldsymbol{C}_{2e}\boldsymbol{C}_{\mathrm{II}e}^T$ is expressible as

$$[\boldsymbol{A}_2]_{mn} = \sum_{p=0}^{N-1} [\boldsymbol{C}_{2e}]_{mp}[\boldsymbol{C}_{\mathrm{II}e}^T]_{pn}, \tag{10}$$

which after substituting the result of Eq. (9) becomes

$$[\boldsymbol{A}_2]_{mn} = \sqrt{\frac{2N}{k_m}} \sum_{p=0}^{N-1} [\boldsymbol{C}_{\mathrm{II}e}]_{mp}[\boldsymbol{C}_{\mathrm{II}e}^T]_{pn}. \tag{11}$$

Because $\boldsymbol{C}_{\mathrm{II}e}$ is unitary, Eq. (11) can be recast as

$$[\boldsymbol{A}_2]_{mn} = \sqrt{\frac{2N}{k_m}}\delta(m-n), \tag{12}$$

where $\delta(m-n)$ is a Kronecker delta function defined by

$$\delta(m-n) = \begin{cases} 1, & m=n \\ 0, & m \neq n. \end{cases} \tag{13}$$

From Eq. (12), $\boldsymbol{A}_2$ is clearly diagonal with the general result for its $m-n$th element given by

$$[\boldsymbol{A}_2]_{mn} = \begin{cases} 2\sqrt{N}, & m=n=0 \\ \sqrt{2N}, & m=n\neq 0 \\ 0, & m\neq n, \end{cases} \tag{14}$$

or more compactly, $\boldsymbol{A}_2 = \sqrt{\frac{2N}{k_m}}\boldsymbol{I}_N$.

Following similar derivations, it follows that $\boldsymbol{A}_4 = \boldsymbol{A}_8 = \sqrt{2N}\boldsymbol{I}_N$, $\boldsymbol{A}_5 = \sqrt{2N}\boldsymbol{I}_{N-1}$, and $\boldsymbol{A}_6 = \sqrt{\frac{2N}{k_m}}\boldsymbol{I}_N$ for any positive $N$ even, and $\boldsymbol{A}_{12} = \boldsymbol{A}_{13} = \boldsymbol{A}_{14} = \boldsymbol{A}_{15} = \sqrt{2N-1}\boldsymbol{I}_{N-1}$ for any positive $N$ odd. These derivations appear in Appendix C. Note $\boldsymbol{A}_2 \neq \boldsymbol{A}_6$ even though both have dimension $N \times N$, because $\boldsymbol{A}_2$ is indexed from 0 to $N-1$ and $\boldsymbol{A}_6$ must be indexed from 1 to $N$ based on the index ranges of the type-II DCT and DST in the trigonometric transform domain.[5]

Thus, diagonal relationships exist for nine out the sixteen DTTs. These diagonal relationships then allow certain of the vector-matrix forms of the symmetric convolution-multiplication property of the DTTs to be recast in terms of unitary transforms.

## New Vector-Matrix Forms of Symmetric Convolution Based on Unitary Transforms

To relate the above results to the vector-matrix forms of the symmetric convolution-multiplication property, consider the following expression which represents just one of the forty cases of symmetric convolution[6] expressed in vector-matrix form:[7]

$$\boldsymbol{d} = \boldsymbol{C}_{2e}^{-1} \boldsymbol{H}_{\boldsymbol{C}_{1e}} \boldsymbol{C}_{2e} \boldsymbol{\theta}. \tag{15}$$

In Eq. (15), the vectors $\boldsymbol{d}$ and $\boldsymbol{\theta}$ represent the input and output sequences, $d(n)$ and $\theta(n)$, and the matrix $\boldsymbol{H}_{\boldsymbol{C}_{1e}} = \mathrm{diag}\{\boldsymbol{C}_{1e} \boldsymbol{h}_{WSWS}^{r}\}$ is the diagonal matrix created by taking the even-length convolutional type-I DCT of the vector $\boldsymbol{h}_{WSWS}^{r}$ which represents the right-half samples of a sequence $h(n)$ having whole-sample symmetry in both the left and right directions.[8] Normally the vector $\boldsymbol{C}_{1e} \boldsymbol{h}_{WSWS}^{r}$ contains $N+1$ samples ranging from 0 to $N$, but here only the first $N$ samples from 0 to $N-1$ need to be retained because the underlying symmetry of the vector $\boldsymbol{C}_{2e} \boldsymbol{\theta}$ forces a zero at $m = N$ which cancels the value of $\boldsymbol{C}_{1e} \boldsymbol{h}_{WSWS}^{r}$ at $m = N$. A more thorough explanation of the underlying symmetry and zero values inherent in symmetric convolution is given in two articles by Martucci.[9] Thus each matrix in Eq. (15) has compatible dimension $N \times N$. Substituting the fact that $\boldsymbol{C}_{2e} = \boldsymbol{A}_2 \boldsymbol{C}_{\mathrm{II}e}$ into Eq. (15) produces

$$\boldsymbol{d} = \boldsymbol{C}_{\mathrm{II}e}^{-1} \boldsymbol{A}_2^{-1} \boldsymbol{H}_{\boldsymbol{C}_{1e}} \boldsymbol{A}_2 \boldsymbol{C}_{\mathrm{II}e} \boldsymbol{\theta}. \tag{16}$$

Recognizing that the three interior matrices in Eq. (16) are diagonal and therefore commute, yields

$$\boldsymbol{d} = \boldsymbol{C}_{\mathrm{II}e}^{-1} \boldsymbol{H}_{\boldsymbol{C}_{1e}} \boldsymbol{C}_{\mathrm{II}e} \boldsymbol{\theta}, \tag{17}$$

which is the desired result based on unitary transform matrices for this particular case of symmetric convolution. A similar result to Eq. (17) based on operator notation first appeared in a conference paper by Martucci.[10] The development presented here follows a matrix approach to derive not only this result but also results based on unitary transform matrices for other cases of symmetric convolution.

Eighteen of the forty cases of symmetric convolution are expressible in terms of unitary transform matrices. The reason not all of the cases can be expressed in terms of unitary transform matrices is because seven of the sixteen DTTs cannot have their convolutional and unitary versions related by a diagonal matrix. Following a similar derivation as that producing Eq. (17), the following eighteen cases are based on unitary transform matrices:

$$\begin{array}{lll}
\boldsymbol{d} = \boldsymbol{S}_{\mathrm{I}e}^{-1} \boldsymbol{H}_{\boldsymbol{C}_{1e}} \boldsymbol{S}_{\mathrm{I}e} \boldsymbol{\theta} & \boldsymbol{d} = \boldsymbol{C}_{\mathrm{II}e}^{-1} \boldsymbol{H}_{\boldsymbol{C}_{1e}} \boldsymbol{C}_{\mathrm{II}e} \boldsymbol{\theta} & \boldsymbol{d} = \boldsymbol{S}_{\mathrm{II}e}^{-1} \boldsymbol{H}_{\boldsymbol{S}_{1e}} \boldsymbol{C}_{\mathrm{II}e} \boldsymbol{\theta} \\
\boldsymbol{d} = \boldsymbol{S}_{\mathrm{II}e}^{-1} \boldsymbol{H}_{\boldsymbol{C}_{1e}} \boldsymbol{S}_{\mathrm{II}e} \boldsymbol{\theta} & \boldsymbol{d} = -\boldsymbol{C}_{\mathrm{II}e}^{-1} \boldsymbol{H}_{\boldsymbol{S}_{1e}} \boldsymbol{S}_{\mathrm{II}e} \boldsymbol{\theta} & \boldsymbol{d} = \boldsymbol{S}_{\mathrm{I}e}^{-1} \boldsymbol{H}_{\boldsymbol{S}_{2e}} \boldsymbol{C}_{\mathrm{II}e} \boldsymbol{\theta} \\
\boldsymbol{d} = \boldsymbol{C}_{\mathrm{IV}e}^{-1} \boldsymbol{H}_{\boldsymbol{C}_{3e}} \boldsymbol{C}_{\mathrm{IV}e} \boldsymbol{\theta} & \boldsymbol{d} = \boldsymbol{S}_{\mathrm{IV}e}^{-1} \boldsymbol{H}_{\boldsymbol{S}_{3e}} \boldsymbol{C}_{\mathrm{IV}e} \boldsymbol{\theta} & \boldsymbol{d} = \boldsymbol{S}_{\mathrm{IV}e}^{-1} \boldsymbol{H}_{\boldsymbol{C}_{3e}} \boldsymbol{S}_{\mathrm{IV}e} \boldsymbol{\theta} \\
\boldsymbol{d} = -\boldsymbol{C}_{\mathrm{IV}e}^{-1} \boldsymbol{H}_{\boldsymbol{S}_{3e}} \boldsymbol{S}_{\mathrm{IV}e} \boldsymbol{\theta} & \boldsymbol{d} = \boldsymbol{S}_{\mathrm{I}o}^{-1} \boldsymbol{H}_{\boldsymbol{C}_{1o}} \boldsymbol{S}_{\mathrm{I}o} \boldsymbol{\theta} & \boldsymbol{d} = \boldsymbol{S}_{\mathrm{II}o}^{-1} \boldsymbol{H}_{\boldsymbol{C}_{2o}} \boldsymbol{S}_{\mathrm{I}o} \boldsymbol{\theta} \\
\boldsymbol{d} = \boldsymbol{S}_{\mathrm{II}o}^{-1} \boldsymbol{H}_{\boldsymbol{C}_{1o}} \boldsymbol{S}_{\mathrm{II}o} \boldsymbol{\theta} & \boldsymbol{d} = \boldsymbol{S}_{\mathrm{I}o}^{-1} \boldsymbol{H}_{\boldsymbol{C}_{2o}} \boldsymbol{S}_{\mathrm{II}o} \boldsymbol{\theta} & \boldsymbol{d} = \boldsymbol{S}_{\mathrm{III}o}^{-1} \boldsymbol{H}_{\boldsymbol{C}_{3o}} \boldsymbol{S}_{\mathrm{III}o} \boldsymbol{\theta} \\
\boldsymbol{d} = \boldsymbol{C}_{\mathrm{IV}o}^{-1} \boldsymbol{H}_{\boldsymbol{C}_{3o}} \boldsymbol{C}_{\mathrm{IV}o} \boldsymbol{\theta} & \boldsymbol{d} = -\boldsymbol{C}_{\mathrm{IV}o}^{-1} \boldsymbol{H}_{\boldsymbol{S}_{4o}} \boldsymbol{S}_{\mathrm{III}o} \boldsymbol{\theta} & \boldsymbol{d} = \boldsymbol{S}_{\mathrm{III}o}^{-1} \boldsymbol{H}_{\boldsymbol{S}_{4o}} \boldsymbol{C}_{\mathrm{IV}o} \boldsymbol{\theta},
\end{array} \tag{18}$$

where the subscripts on the $\boldsymbol{H}$ matrices indicate the type of DTT applied to the right-half samples of the sequence $h(n)$ in each case. All the derivations for the cases in Eq. (18) appear in Appendix D. The derivations for the cases with identical forward and inverse unitary transforms are straightforward. The derivations for the odd-length cases with different forward and inverse transforms occur because the matrices $\boldsymbol{A}_{12} - \boldsymbol{A}_{15}$ relating the odd cases are all identical. The remaining derivations, *i.e.* those for the even-length cases with different forward and inverse transforms, use either the fact that the relating matrices $\boldsymbol{A}_4$ and $\boldsymbol{A}_8$ are identically equal, or they use the fact that the matrices $\boldsymbol{A}_2$, $\boldsymbol{A}_5$, and $\boldsymbol{A}_6$ are identical for index values of 1 to $N-1$.

Equation (18) presents the symmetric convolution-multiplication property of DTTs based on unitary rather than convolutional transforms for the eighteen out of forty total cases where it exists. The results based on unitary rather than convolutional transforms are significant because many applications require the unitary version of the transform. For example, a great deal of hardware on the market today performs image coding based on unitary versions of the DCT and DST. Now it is possible to perform filtering in the transform domain of the DTTs, without having to first convert between the convolutional and unitary versions of the transforms.

The following chapter shows how this new property has applications to the image reconstruction problem imposed by imaging through turbulence.

**Notes**

[1] Thomas M. Foltz, Byron M. Welsh, and Courtney D. Holmberg, "Symmetric Convolution Using Unitary Transform Matrices," submitted to *IEEE Transactions on Signal Processing.*

[2] Zhongde Wang and B.R. Hunt, "The Discrete W Transform," *Applied Mathematics and Computation* 16, no. 1 (January 1985): 33–35.

## Notes

[3] Stephen A. Martucci, "Symmetric Convolution and the Discrete Sine and Cosine Transforms," *IEEE Transactions on Signal Processing* 42, no. 5 (May 1994): 1040, 1050.

[4] Wang and Hunt.

[5] Ibid., and Martucci.

[6] Martucci, 1038–1051.

[7] Foltz and Welsh, "Symmetric Convolution of Asymmetric Multidimensional Sequences Using Discrete Trigonometric Transforms," to appear in *IEEE Transactions on Image Processing* 8, no. 5 (May 1999).

[8] Martucci, 1046–1048.

[9] Ibid., 1038–1051, and

Martucci, "Digital Filtering of Images Using the Discrete Sine and Cosine Transforms," *Optical Engineering* 35, no. 1 (January 1996): 119–127.

[10] Martucci, "Image Resizing in the Discrete Cosine Transform Domain," in *Proceedings of the IEEE International Conference on Image Processing*, vol. 2, Washington, D.C., (October 1995): 244–247.

# Chapter 5

# Proposal for Near-Real-Time Imaging System

To the casual observer, perhaps unfamiliar with the mathematical subtleties presented in the previous chapter, it might appear that these preliminary results are insignificant in that they simply replace a few numeric subscripts in a handful of equations with Roman numeral subscripts. On the contrary, the meaning behind the change of subscripts is what is significant. However, even the change itself would be purely a mathematical contrivance were it not for the potential impact the change has to improve systems in the real world.

This chapter presents some ideas for ways to improve existing methods of imaging through turbulence. The results derived in this paper can not only help the performance of Air Force systems using adaptive optics, but they also pose an even greater benefit to systems that perform image processing to correct for turbulence directly.

The techniques developed here can increase the speed of transform domain calculations used to correct for turbulence in adaptive optics systems. The increase in speed arises because for real sequences, like the pixels of an image, the trigonometric transform domain coefficients are also all real, where they are complex in the Fourier domain. Fast algorithms exist for the discrete trigonometric transforms[1] that operate with the same number of floating point operations as fast Fourier transforms.[2] These algorithms use on the order of $N \log_2 N$ operations to compute the transform of an image with $N$ pixels. It follows in a straightforward manner that it is easier to perform filtering by using $N \log_2 N$ operations to calculate the forward transform, calculating $N$ multiplications in the transform domain, and then performing $N \log_2 N$ operations to calculate the inverse transform, than it is to compute the $2N^2$ operations needed to perform convolution directly. [Note the superscript '2' indicates a squaring operation and not an endnote.]

The discrete trigonometric transforms present an additional savings in computational complexity over discrete Fourier transforms, because the algorithms use all real arithmetic for a real-valued image. Complex additions require twice the number of floating point operations as real additions and complex multiplications typically require six times the number of floating point operations as real multiplications. Because images that are in general asymmetric need to be decomposed into their four underlying symmetric parts, the overall computational savings amounts to about two-thirds the speed of existing complex-arithmetic algorithms.[3]

Embedded into the processor of an adaptive optics system, algorithms based on the unitary versions of the discrete trigonometric transforms could speed up the refresh times of the system, giving it more fidelity. Being able to process measurements from wavefront sensor readings in two-thirds the existing time could boost the measurement rate from 100 to 150 Hz. This increase would allow the system to adapt more quickly to changing atmospheric conditions.

The results of the previous chapter can also improve techniques that perform image processing to restore degraded images. Image processing systems that measure the effects of atmospheric perturbations and then use a computer to correct for the effects of the distortion can also operate two-thirds faster than existing systems by using trigonometric rather than Fourier processing. Other image processing techniques that do not measure the turbulence, but instead apply nonlinear iterative algorithms to reproduce a turbulence-compensated image, stand to benefit as well. The overall algorithms will take less time to converge because each iteration will require less processing time, and they may converge in fewer iterations because trigonometric transforms provide better scalar approximations than other transforms.[4]

Linear image processing systems that compute their estimated objects directly may stand to show the most benefit from these new results by using unitary trigonometric transforms to compute the convolution of an incoming image with the two dimensional impulse response of a linear reconstruction filter in the trigonometric transform domain. Since hardware based on the unitary versions of the discrete trigonometric transforms is readily available, it is conceivable that future applications might lend themselves to a real-time hardware systems rather than delayed computer post-processing. A hardware-based system would have tremendous advantages in speed of calculation, and could be prototyped in a laboratory using off-the-shelf integrated circuits to perform the trigonometric transforms.

The improvements suggested here for the next generation of ground-based optical sensors are well grounded in supporting military and national strategic aims. The ideas presented in this paper stand to help further develop the Air Force's core competency of information superiority[5] by collecting vital information on our adversaries' space-borne systems. These concepts also fit within the National Military Strategy's charter to "**shape** the international environment," "**respond** to … crises," and "**prepare now** for an uncertain future."[6] Part of shaping the international environment calls for "preventing or reducing conflicts or threats,"[7] and specifically mentions reducing the development of technology related to weapons of mass destruction.[8] The increased quality of the images generated by this proposed system would help national level strategists to verify compliance with existing treaties on nonproliferation of space-based weapons and enable them to respond appropriately. Joint Vision 2010[9] lists information superiority and technological innovations—two areas to which this research relates—as supporting concepts enabling the military forces of the future to achieve full spectrum dominance during peacetime and war. All of these military concepts derive from the National Security Strategy Document, which discusses intelligence, surveillance, and reconnaissance and space as two overarching capabilities that help the U.S. advance its national interests.[10]

Looking years ahead into the future, should space-based weapons become the norm, then the system proposed here could provide space warfighters with near-real-time battle damage assessment following attacks on enemy or friendly space systems. On a final note, besides their applications to optical systems, the technical results of this research can also benefit other areas such as communications, signal processing, and control systems applications, even though the original focus of these efforts was derived specifically for image reconstruction.

## Notes

[1] See for example:

Zhongde Wang, "Fast Algorithms for the Discrete W Transform and for the Discrete Fourier Transform," *IEEE Transactions on Acoustics, Speech, and Signal Processing* ASSP-32, no. 4 (August 1984): 803–816.

Anil K. Jain, *Fundamentals of Digital Image Processing*. (Englewood Cliffs, N.J.: Prentice-Hall, 1989), Chapter 8, 152–153.

and

## Notes

K.R. Rao and P. Yip, *Discrete Cosine Transform: Algorithms, Advantages, Applications*. (San Diego: Academic Press, 1990), Chapter 4, 48–87.

[2] Alan V. Oppenheim and Ronald W. Schafer, *Digital Signal Processing*. (Englewood Cliffs, N.J.: Prentice-Hall, 1975), Chapter 6, 284–336.

[3] Thomas M. Foltz and Byron M. Welsh, "Symmetric Convolution of Asymmetric Multidimensional Sequences Using Discrete Trigonometric Transforms," to appear in *IEEE Transactions on Image Processing* 8, no. 5 (May 1999).

[4] Jain, 153–154.

[5] Air Force Doctrine Document (AFDD) 1. *Air Force Basic Doctrine,* September 1997, 31–32.

[6] *National Military Strategy of the United States of America,* September 1997, 1.

[7] Ibid., 13.

[8] Ibid., 14.

[9] *Joint Vision 2010,* not dated, 26.

[10] *A National Security Strategy for a New Century*, The White House, October 1998, 24–26.

# Chapter 6

# Conclusion

This research paper has documented a fundamentally new principle regarding image reconstruction. It has presented general background information on how the Air Force images space-borne objects from the ground. It has introduced readers to the mathematical concepts of image reconstruction, symmetric convolution and the discrete trigonometric transforms, and has shown how symmetric convolution can be used to perform image reconstruction. The results presented in this paper that relate the convolutional and unitary trigonometric transforms and present unitary transform based versions of the symmetric convolution-multiplication property demonstrate a new contribution to the field.

This paper has proposed that image processing algorithms based on unitary trigonometric transforms and symmetric convolution would enhance existing image reconstruction systems. Although symmetric convolution is a fairly recent discovery[1] that has previously been applied to image reconstruction,[2] it relies on a special convolutional form for each of the sixteen discrete trigonometric transforms. The results of this research cast the symmetric convolution-multiplication property of the discrete trigonometric transforms into the more traditional unitary versions of the discrete trigonometric transforms. By performing symmetric convolution with unitary rather than convolutional transforms, faster computational and even direct hardware realizations of image reconstruction filters are possible based on existing discrete cosine transform chips. These hardware realizations can then be used to improve the capability of ground-based imaging systems that surveil space-borne objects, an Air Force function well grounded in service and military doctrine as well as military and national strategy.

Now that the symmetric convolution-multiplication property exists for unitary transforms, some directions for future research might include recasting existing inverse and scalar Wiener filters[3] in terms of the new transforms. Another limitation that also needs to be overcome through future research efforts is to expand the noise model upon which the scalar Wiener filter is based to include photon-dependent Poisson noise.[4] Enhancing the noise model will make these already improved techniques even more robust.

## Notes

[1] Stephen A. Martucci, "Symmetric Convolution and the Discrete Sine and Cosine Transforms," *IEEE Transactions on Signal Processing* 42, no. 5 (May 1994): 1038–1051.

[2] T.M. Foltz and B.M. Welsh, "Image Reconstruction Using Symmetric Convolution and Discrete Trigonometric Transforms," *Journal of the Optical Society of America A* 15, no. 11 (November 1998): 2827–2840.

[3] Ibid.

[4] Michael C. Roggemann and Byron M. Welsh, *Imaging Through Turbulence*. (Boca Raton, Fla.: CRC Press, 1996), 44–54.

## Appendix A

# Convolutional and Unitary Discrete Trigonometric Transforms

This appendix provides definitions of the sixteen convolutional versions of the discrete trigonometric transforms (DTTs) and the sixteen unitary versions of the DTTs.

Martucci[1] defines the sixteen convolutional versions of the discrete cosine and sine transforms (DCTs and DSTs) by their $m-n$th elements as:

$$[\boldsymbol{C}_{1e}]_{mn} = 2k_n \cos\left(\frac{\pi mn}{N}\right), \qquad m, n = 0, 1, \ldots, N, \tag{A1}$$

$$[\boldsymbol{C}_{2e}]_{mn} = 2\cos\left(\frac{\pi m(n+\frac{1}{2})}{N}\right), \qquad m, n = 0, 1, \ldots, N-1, \tag{A2}$$

$$[\boldsymbol{C}_{3e}]_{mn} = 2k_n \cos\left(\frac{\pi (m+\frac{1}{2})n}{N}\right), \qquad m, n = 0, 1, \ldots, N-1, \tag{A3}$$

$$[\boldsymbol{C}_{4e}]_{mn} = 2\cos\left(\frac{\pi (m+\frac{1}{2})(n+\frac{1}{2})}{N}\right), \qquad m, n = 0, 1, \ldots, N-1, \tag{A4}$$

$$[\boldsymbol{S}_{1e}]_{mn} = 2\sin\left(\frac{\pi mn}{N}\right), \qquad m, n = 1, 2, \ldots, N-1, \tag{A5}$$

$$[\boldsymbol{S}_{2e}]_{mn} = 2\sin\left(\frac{\pi m(n+\frac{1}{2})}{N}\right), \qquad \begin{array}{l} m = 1, 2, \ldots, N \\ n = 0, 1, \ldots, N-1, \end{array} \tag{A6}$$

$$[\boldsymbol{S}_{3e}]_{mn} = 2k_n \sin\left(\frac{\pi (m+\frac{1}{2})n}{N}\right), \qquad \begin{array}{l} m = 0, 1, \ldots, N-1 \\ n = 1, 2, \ldots, N, \end{array} \tag{A7}$$

$$[\boldsymbol{S}_{4e}]_{mn} = 2\sin\left(\frac{\pi(m+\frac{1}{2})(n+\frac{1}{2})}{N}\right), \qquad m, n = 0, 1, \ldots, N-1, \qquad \text{(A8)}$$

$$[\boldsymbol{C}_{1o}]_{mn} = 2k_n \cos\left(\frac{2\pi mn}{2N-1}\right), \qquad m, n = 0, 1, \ldots, N-1, \qquad \text{(A9)}$$

$$[\boldsymbol{C}_{2o}]_{mn} = 2l_n \cos\left(\frac{2\pi m(n+\frac{1}{2})}{2N-1}\right), \qquad m, n = 0, 1, \ldots, N-1, \qquad \text{(A10)}$$

$$[\boldsymbol{C}_{3o}]_{mn} = 2k_n \cos\left(\frac{2\pi(m+\frac{1}{2})n}{2N-1}\right), \qquad m, n = 0, 1, \ldots, N-1, \qquad \text{(A11)}$$

$$[\boldsymbol{C}_{4o}]_{mn} = 2\cos\left(\frac{2\pi(m+\frac{1}{2})(n+\frac{1}{2})}{2N-1}\right), \qquad m, n = 0, 1, \ldots, N-2, \qquad \text{(A12)}$$

$$[\boldsymbol{S}_{1o}]_{mn} = 2\sin\left(\frac{2\pi mn}{2N-1}\right), \qquad m, n = 1, 2, \ldots, N-1, \qquad \text{(A13)}$$

$$[\boldsymbol{S}_{2o}]_{mn} = 2\sin\left(\frac{2\pi m(n+\frac{1}{2})}{2N-1}\right), \qquad \begin{array}{l} m = 1, 2, \ldots, N-1 \\ n = 0, 1, \ldots, N-2, \end{array} \qquad \text{(A14)}$$

$$[\boldsymbol{S}_{3o}]_{mn} = 2\sin\left(\frac{2\pi(m+\frac{1}{2})n}{2N-1}\right), \qquad \begin{array}{l} m = 0, 1, \ldots, N-2 \\ n = 1, 2, \ldots, N-1, \end{array} \qquad \text{(A15)}$$

and

$$[\boldsymbol{S}_{4o}]_{mn} = 2l_n \sin\left(\frac{2\pi(m+\frac{1}{2})(n+\frac{1}{2})}{2N-1}\right), \qquad m, n = 0, 1, \ldots, N-1. \qquad \text{(A16)}$$

The constants in Eqs. (A1)–(A16) are defined by

$$k_p = \begin{cases} \frac{1}{2}, & p = 0, N \\ 1, & \text{otherwise} \end{cases} \qquad \text{and} \qquad l_p = \begin{cases} \frac{1}{2}, & p = N-1 \\ 1, & \text{otherwise,} \end{cases} \qquad \text{(A17)}$$

where $p$ can be either $m$ or $n$. The matrices denoted by $\boldsymbol{C}$ and $\boldsymbol{S}$ represent DCT and DST matrices respectively, the numeric subscripts '1–4' represent types I–IV for the convolutional versions of the DTTs, and the subscripts '*e*' and '*o*' denote even and odd length versions of the DTT matrices.

Wang and Hunt[2] define the sixteen unitary versions of the DTTs by their $m-n$th elements as:

$$[\boldsymbol{C}_{\mathrm{I}e}]_{mn}=\sqrt{\frac{2}{N}k_m k_n}\cos\left(\frac{\pi mn}{N}\right), \qquad m,n=0,1,\ldots,N, \qquad \text{(A18)}$$

$$[\boldsymbol{C}_{\mathrm{II}e}]_{mn}=\sqrt{\frac{2}{N}k_m}\cos\left(\frac{\pi m(n+\frac{1}{2})}{N}\right), \qquad m,n=0,1,\ldots,N-1, \qquad \text{(A19)}$$

$$[\boldsymbol{C}_{\mathrm{III}e}]_{mn}=\sqrt{\frac{2}{N}k_n}\cos\left(\frac{\pi(m+\frac{1}{2})n}{N}\right), \qquad m,n=0,1,\ldots,N-1, \qquad \text{(A20)}$$

$$[\boldsymbol{C}_{\mathrm{IV}e}]_{mn}=\sqrt{\frac{2}{N}}\cos\left(\frac{\pi(m+\frac{1}{2})(n+\frac{1}{2})}{N}\right), \qquad m,n=0,1,\ldots,N-1, \qquad \text{(A21)}$$

$$[\boldsymbol{S}_{\mathrm{I}e}]_{mn}=\sqrt{\frac{2}{N}}\sin\left(\frac{\pi mn}{N}\right), \qquad m,n=1,2,\ldots,N-1, \qquad \text{(A22)}$$

$$[\boldsymbol{S}_{\mathrm{II}e}]_{mn}=\sqrt{\frac{2}{N}k_m}\sin\left(\frac{\pi m(n+\frac{1}{2})}{N}\right), \qquad \begin{array}{l} m=1,2,\ldots,N \\ n=0,1,\ldots,N-1, \end{array} \qquad \text{(A23)}$$

$$[\boldsymbol{S}_{\mathrm{III}e}]_{mn}=\sqrt{\frac{2}{N}k_n}\sin\left(\frac{\pi(m+\frac{1}{2})n}{N}\right), \qquad \begin{array}{l} m=0,1,\ldots,N-1 \\ n=1,2,\ldots,N, \end{array} \qquad \text{(A24)}$$

$$[\boldsymbol{S}_{\mathrm{IV}e}]_{mn}=\sqrt{\frac{2}{N}}\sin\left(\frac{\pi(m+\frac{1}{2})(n+\frac{1}{2})}{N}\right), \qquad m,n=0,1,\ldots,N-1, \qquad \text{(A25)}$$

$$[\boldsymbol{C}_{\mathrm{I}o}]_{mn}=2\sqrt{\frac{k_m k_n}{2N-1}}\cos\left(\frac{2\pi mn}{2N-1}\right), \qquad m,n=0,1,\ldots,N-1, \qquad \text{(A26)}$$

$$[\boldsymbol{C}_{\mathrm{II}o}]_{mn}=2\sqrt{\frac{k_m l_n}{2N-1}}\cos\left(\frac{2\pi m(n+\frac{1}{2})}{2N-1}\right), \qquad m,n=0,1,\ldots,N-1, \qquad \text{(A27)}$$

$$[\boldsymbol{C}_{\mathrm{III}o}]_{mn}=2\sqrt{\frac{l_m k_n}{2N-1}}\cos\left(\frac{2\pi(m+\frac{1}{2})n}{2N-1}\right), \qquad m,n=0,1,\ldots,N-1, \qquad \text{(A28)}$$

$$[\boldsymbol{C}_{\mathrm{IV}o}]_{mn}=\frac{2}{\sqrt{2N-1}}\cos\left(\frac{2\pi(m+\frac{1}{2})(n+\frac{1}{2})}{2N-1}\right), \qquad m,n=0,1,\ldots,N-2, \qquad \text{(A29)}$$

$$[\boldsymbol{S}_{\mathrm{I}o}]_{mn} = \frac{2}{\sqrt{2N-1}} \sin\left(\frac{2\pi mn}{2N-1}\right), \qquad m, n = 1, 2, \ldots, N-1, \tag{A30}$$

$$[\boldsymbol{S}_{\mathrm{II}o}]_{mn} = \frac{2}{\sqrt{2N-1}} \sin\left(\frac{2\pi m(n+\frac{1}{2})}{2N-1}\right), \qquad \begin{array}{l} m = 1, 2, \ldots, N-1 \\ n = 0, 1, \ldots, N-2, \end{array} \tag{A31}$$

$$[\boldsymbol{S}_{\mathrm{III}o}]_{mn} = \frac{2}{\sqrt{2N-1}} \sin\left(\frac{2\pi (m+\frac{1}{2})n}{2N-1}\right), \qquad \begin{array}{l} m = 0, 1, \ldots, N-2 \\ n = 1, 2, \ldots, N-1, \end{array} \tag{A32}$$

and

$$[\boldsymbol{S}_{\mathrm{IV}o}]_{mn} = 2\sqrt{\frac{l_m l_n}{2N-1}} \sin\left(\frac{2\pi (m+\frac{1}{2})(n+\frac{1}{2})}{2N-1}\right), \qquad m, n = 0, 1, \ldots, N-1. \tag{A33}$$

The definitions in Eqs. (A18)–(A33) differ slightly in appearance from those given by Wang and Hunt,[3] but they produce exactly the same unitary transform matrices. The differences arise because Eqs. (A18)–(A33) use the constants given by Eq. (A17) and the indexing on certain of the DST matrices is different. The only reason for defining the DTT matrices differently is to allow a more direct comparison to Martucci's convolutional versions of the DTTs.[4]

## Notes

[1] Stephen A. Martucci, "Symmetric Convolution and the Discrete Sine and Cosine Transforms," *IEEE Transactions on Signal Processing* 42, no. 5 (May 1994): 1038–1051.

[2] Zhongde Wang and B.R. Hunt, "The Discrete W Transform," *Applied Mathematics and Computation* 16, no. 1 (January 1985): 33–35.

[3] Ibid.

[4] Martucci, 1050.

# Appendix B

## Forty Cases of Symmetric Convolution

This appendix lists the forty cases of symmetric convolution.[1] The cases, appearing in vector-matrix form,[2] are:

| | |
|---|---|
| 1.) $\boldsymbol{d} = \boldsymbol{C}_{1e}^{-1} H_{\boldsymbol{C}_{1e}} \boldsymbol{C}_{1e} \boldsymbol{\theta}$ | 21.) $\boldsymbol{d} = \boldsymbol{C}_{1o}^{-1} H_{\boldsymbol{C}_{1o}} \boldsymbol{C}_{1o} \boldsymbol{\theta}$ |
| 2.) $\boldsymbol{d} = \boldsymbol{S}_{1e}^{-1} H_{\boldsymbol{C}_{1e}} \boldsymbol{S}_{1e} \boldsymbol{\theta}$ | 22.) $\boldsymbol{d} = \boldsymbol{S}_{1o}^{-1} H_{\boldsymbol{C}_{1o}} \boldsymbol{S}_{1o} \boldsymbol{\theta}$ |
| 3.) $\boldsymbol{d} = -\boldsymbol{C}_{1e}^{-1} H_{\boldsymbol{S}_{1e}} \boldsymbol{S}_{1e} \boldsymbol{\theta}$ | 23.) $\boldsymbol{d} = -\boldsymbol{C}_{1o}^{-1} H_{\boldsymbol{S}_{1o}} \boldsymbol{S}_{1o} \boldsymbol{\theta}$ |
| 4.) $\boldsymbol{d} = \boldsymbol{C}_{2e}^{-1} H_{\boldsymbol{C}_{1e}} \boldsymbol{C}_{2e} \boldsymbol{\theta}$ | 24.) $\boldsymbol{d} = \boldsymbol{C}_{2o}^{-1} H_{\boldsymbol{C}_{2o}} \boldsymbol{C}_{1o} \boldsymbol{\theta}$ |
| 5.) $\boldsymbol{d} = \boldsymbol{S}_{2e}^{-1} H_{\boldsymbol{S}_{1e}} \boldsymbol{C}_{2e} \boldsymbol{\theta}$ | 25.) $\boldsymbol{d} = \boldsymbol{S}_{2o}^{-1} H_{\boldsymbol{C}_{2o}} \boldsymbol{S}_{1o} \boldsymbol{\theta}$ |
| 6.) $\boldsymbol{d} = \boldsymbol{S}_{2e}^{-1} H_{\boldsymbol{C}_{1e}} \boldsymbol{S}_{2e} \boldsymbol{\theta}$ | 26.) $\boldsymbol{d} = \boldsymbol{S}_{2o}^{-1} H_{\boldsymbol{C}_{1o}} \boldsymbol{S}_{2o} \boldsymbol{\theta}$ |
| 7.) $\boldsymbol{d} = -\boldsymbol{C}_{2e}^{-1} H_{\boldsymbol{S}_{1e}} \boldsymbol{S}_{2e} \boldsymbol{\theta}$ | 27.) $\boldsymbol{d} = -\boldsymbol{C}_{2o}^{-1} H_{\boldsymbol{S}_{1o}} \boldsymbol{S}_{2o} \boldsymbol{\theta}$ |
| 8.) $\boldsymbol{d} = \boldsymbol{C}_{1e}^{-1} H_{\boldsymbol{C}_{2e}} \boldsymbol{C}_{2e} \boldsymbol{\theta}$ | 28.) $\boldsymbol{d} = \boldsymbol{C}_{1o}^{-1} H_{\boldsymbol{C}_{2o}} \boldsymbol{C}_{2o} \boldsymbol{\theta}$ |
| 9.) $\boldsymbol{d} = \boldsymbol{S}_{1e}^{-1} H_{\boldsymbol{S}_{2e}} \boldsymbol{C}_{2e} \boldsymbol{\theta}$ | 29.) $\boldsymbol{d} = \boldsymbol{S}_{1o}^{-1} H_{\boldsymbol{C}_{2o}} \boldsymbol{S}_{2o} \boldsymbol{\theta}$ |
| 10.) $\boldsymbol{d} = -\boldsymbol{C}_{1e}^{-1} H_{\boldsymbol{S}_{2e}} \boldsymbol{S}_{2e} \boldsymbol{\theta}$ | 30.) $\boldsymbol{d} = -\boldsymbol{C}_{1o}^{-1} H_{\boldsymbol{S}_{2o}} \boldsymbol{S}_{2o} \boldsymbol{\theta}$ |
| 11.) $\boldsymbol{d} = \boldsymbol{C}_{3e}^{-1} H_{\boldsymbol{C}_{3e}} \boldsymbol{C}_{3e} \boldsymbol{\theta}$ | 31.) $\boldsymbol{d} = \boldsymbol{C}_{3o}^{-1} H_{\boldsymbol{C}_{3o}} \boldsymbol{C}_{3o} \boldsymbol{\theta}$ |
| 12.) $\boldsymbol{d} = \boldsymbol{S}_{3e}^{-1} H_{\boldsymbol{C}_{3e}} \boldsymbol{S}_{3e} \boldsymbol{\theta}$ | 32.) $\boldsymbol{d} = \boldsymbol{S}_{3o}^{-1} H_{\boldsymbol{C}_{3o}} \boldsymbol{S}_{3o} \boldsymbol{\theta}$ |
| 13.) $\boldsymbol{d} = -\boldsymbol{C}_{3e}^{-1} H_{\boldsymbol{S}_{3e}} \boldsymbol{S}_{3e} \boldsymbol{\theta}$ | 33.) $\boldsymbol{d} = -\boldsymbol{C}_{3o}^{-1} H_{\boldsymbol{S}_{3o}} \boldsymbol{S}_{3o} \boldsymbol{\theta}$ |
| 14.) $\boldsymbol{d} = \boldsymbol{C}_{4e}^{-1} H_{\boldsymbol{C}_{3e}} \boldsymbol{C}_{4e} \boldsymbol{\theta}$ | 34.) $\boldsymbol{d} = \boldsymbol{C}_{4o}^{-1} H_{\boldsymbol{C}_{4o}} \boldsymbol{C}_{3o} \boldsymbol{\theta}$ |
| 15.) $\boldsymbol{d} = \boldsymbol{S}_{4e}^{-1} H_{\boldsymbol{S}_{3e}} \boldsymbol{C}_{4e} \boldsymbol{\theta}$ | 35.) $\boldsymbol{d} = \boldsymbol{S}_{4o}^{-1} H_{\boldsymbol{C}_{4o}} \boldsymbol{S}_{3o} \boldsymbol{\theta}$ |
| 16.) $\boldsymbol{d} = \boldsymbol{S}_{4e}^{-1} H_{\boldsymbol{C}_{3e}} \boldsymbol{S}_{4e} \boldsymbol{\theta}$ | 36.) $\boldsymbol{d} = \boldsymbol{S}_{4o}^{-1} H_{\boldsymbol{S}_{4o}} \boldsymbol{C}_{3o} \boldsymbol{\theta}$ |
| 17.) $\boldsymbol{d} = -\boldsymbol{C}_{4e}^{-1} H_{\boldsymbol{S}_{3e}} \boldsymbol{S}_{4e} \boldsymbol{\theta}$ | 37.) $\boldsymbol{d} = -\boldsymbol{C}_{4o}^{-1} H_{\boldsymbol{S}_{4o}} \boldsymbol{S}_{3o} \boldsymbol{\theta}$ |
| 18.) $\boldsymbol{d} = \boldsymbol{C}_{3e}^{-1} H_{\boldsymbol{C}_{4e}} \boldsymbol{C}_{4e} \boldsymbol{\theta}$ | 38.) $\boldsymbol{d} = \boldsymbol{C}_{3o}^{-1} H_{\boldsymbol{C}_{4o}} \boldsymbol{C}_{4o} \boldsymbol{\theta}$ |
| 19.) $\boldsymbol{d} = \boldsymbol{S}_{3e}^{-1} H_{\boldsymbol{S}_{4e}} \boldsymbol{C}_{4e} \boldsymbol{\theta}$ | 39.) $\boldsymbol{d} = \boldsymbol{S}_{3o}^{-1} H_{\boldsymbol{S}_{4o}} \boldsymbol{C}_{4o} \boldsymbol{\theta}$ |
| 20.) $\boldsymbol{d} = -\boldsymbol{C}_{3e}^{-1} H_{\boldsymbol{S}_{4e}} \boldsymbol{S}_{4e} \boldsymbol{\theta}$ | 40.) $\boldsymbol{d} = -\boldsymbol{C}_{3o}^{-1} H_{\boldsymbol{S}_{4o}} \boldsymbol{S}_{4o} \boldsymbol{\theta}$. (B1) |

## Notes

[1] Stephen A. Martucci, "Symmetric Convolution and the Discrete Sine and Cosine Transforms," *IEEE Transactions on Signal Processing* 42, no. 5 (May 1994): 1050.

[2] Maj Thomas M. Foltz, "Trigonometric Transforms for Image Reconstruction," Ph.D. Dissertation, AFIT/DS/ENG/98-04. Air Force Institute of Technology (AETC), Wright-Patterson AFB, Ohio, June 1998, 1–122.

and

Foltz and B.M. Welsh, "Symmetric Convolution of Asymmetric Multidimensional Sequences Using Discrete Trigonometric Transforms," to appear in *IEEE Transactions on Image Processing* 8, no. 5 (May1999).

## Appendix C

# Derivation of Diagonal Relationships between Convolutional and Unitary Transform Matrices

This appendix displays derivations of the nine diagonal relationships that exist between the convolutional and unitary versions of the discrete cosine and sine transforms (DCTs and DSTs). The derivation in Chapter 4 showing that the matrix $\boldsymbol{A}_2$ is diagonal is repeated here for completeness.

### Diagonal Relationship for Type-II Even-Length DCT

Consider the matrix $\boldsymbol{A}_2 = \boldsymbol{C}_{2e}\boldsymbol{C}_{\mathrm{II}e}^T$. Recall the definitions for the $m-n$th elements of the $N \times N$ type-II even-length DCT matrices from Appendix A:

$$[\boldsymbol{C}_{2e}]_{mn} = 2\cos\left(\frac{\pi m(n+\frac{1}{2})}{N}\right), \tag{C1}$$

and

$$[\boldsymbol{C}_{\mathrm{II}e}]_{mn} = \sqrt{\frac{2}{N}k_m}\cos\left(\frac{\pi m(n+\frac{1}{2})}{N}\right), \tag{C2}$$

for $m, n = 0, 1, \ldots, N-1$. The constant, $k_m$, in Eq. (C2) is defined in Eq. (A17). It follows from Eqs. (C1) and (C2) that

$$[\boldsymbol{C}_{2e}]_{mn} = \sqrt{\frac{2N}{k_m}}[\boldsymbol{C}_{\mathrm{II}e}]_{mn}. \tag{C3}$$

The $m-n$th element of the product $\boldsymbol{A}_2 = \boldsymbol{C}_{2e}\boldsymbol{C}_{\mathrm{II}e}^T$ is expressible as

$$[\boldsymbol{A}_2]_{mn} = \sum_{p=0}^{N-1} [\boldsymbol{C}_{2e}]_{mp} [\boldsymbol{C}_{\mathrm{II}e}^T]_{pn}, \tag{C4}$$

which after substituting the result of Eq. (C3) becomes

$$[\boldsymbol{A}_2]_{mn} = \sqrt{\frac{2N}{k_m}} \sum_{p=0}^{N-1} [\boldsymbol{C}_{\mathrm{II}e}]_{mp} [\boldsymbol{C}_{\mathrm{II}e}^T]_{pn}. \tag{C5}$$

Because the matrix $\boldsymbol{C}_{\mathrm{II}e}$ is unitary, Eq. (C5) can be recast as

$$[\boldsymbol{A}_2]_{mn} = \sqrt{\frac{2N}{k_m}}\delta(m-n), \tag{C6}$$

where $\delta(m-n)$ is a Kronecker delta function. From Eq. (C6), $\boldsymbol{A}_2$ is clearly diagonal with the general result for its $m-n$th element given by

$$[\boldsymbol{A}_2]_{mn} = \begin{cases} 2\sqrt{N}, & m=n=0 \\ \sqrt{2N}, & m=n\neq 0 \\ 0, & m\neq n, \end{cases} \tag{C7}$$

or more compactly, $\boldsymbol{A}_2 = \sqrt{\frac{2N}{k_m}}\boldsymbol{I}$.

## Diagonal Relationship for Type-IV Even-Length DCT

Consider the matrix $\boldsymbol{A}_4 = \boldsymbol{C}_{4e}\boldsymbol{C}_{\mathrm{IV}e}^T$. Recall the definitions for the $m-n$th elements of the $N\times N$ type-IV even-length DCT matrices from Appendix A:

$$[\boldsymbol{C}_{4e}]_{mn} = 2\cos\left(\frac{\pi(m+\frac{1}{2})(n+\frac{1}{2})}{N}\right), \tag{C8}$$

and

$$[\boldsymbol{C}_{\mathrm{IV}e}]_{mn} = \sqrt{\frac{2}{N}}\cos\left(\frac{\pi(m+\frac{1}{2})(n+\frac{1}{2})}{N}\right), \tag{C9}$$

for $m, n = 0, 1, \ldots, N-1.$ It follows from Eqs. (C8) and (C9) that

$$[\boldsymbol{C}_{4e}]_{mn} = \sqrt{2N}[\boldsymbol{C}_{\mathrm{IV}e}]_{mn}. \tag{C10}$$

The $m-n$th element of the product $\boldsymbol{A}_4 = \boldsymbol{C}_{4e}\boldsymbol{C}_{\mathrm{IV}e}^T$ is expressible as

$$[\boldsymbol{A}_4]_{mn} = \sum_{p=0}^{N-1}[\boldsymbol{C}_{4e}]_{mp}[\boldsymbol{C}_{\mathrm{IV}e}^T]_{pn}, \tag{C11}$$

which after substituting the result of Eq. (C10) becomes

$$[\boldsymbol{A}_4]_{mn} = \sqrt{2N}\sum_{p=0}^{N-1}[\boldsymbol{C}_{\mathrm{IV}e}]_{mp}[\boldsymbol{C}_{\mathrm{IV}e}^T]_{pn}. \tag{C12}$$

Because the matrix $\boldsymbol{C}_{\mathrm{IV}e}$ is unitary, Eq. (C12) can be recast as

$$[\boldsymbol{A}_4]_{mn} = \sqrt{2N}\delta(m-n), \tag{C13}$$

from which it is clear that $\boldsymbol{A}_4 = \sqrt{2N}\boldsymbol{I}.$

## Diagonal Relationship for Type-I Even-Length DST

Consider the matrix $\boldsymbol{A}_5 = \boldsymbol{S}_{1e}\boldsymbol{S}_{\mathrm{I}e}^T.$ Recall the definitions for the $m-n$th elements of the $N-1\times N-1$ type-I even-length DST matrices from Appendix A:

$$[\boldsymbol{S}_{1e}]_{mn} = 2\sin\left(\frac{\pi mn}{N}\right), \tag{C14}$$

and

$$[\boldsymbol{S}_{\mathrm{I}e}]_{mn} = \sqrt{\frac{2}{N}}\sin\left(\frac{\pi mn}{N}\right), \tag{C15}$$

for $m, n = 1, 2, \ldots, N-1.$ It follows from Eqs. (C14) and (C15) that

$$[\boldsymbol{S}_{1e}]_{mn} = \sqrt{2N}[\boldsymbol{S}_{\mathrm{I}e}]_{mn}. \tag{C16}$$

The $m-n$th element of the product $\boldsymbol{A}_5 = \boldsymbol{S}_{1e}\boldsymbol{S}_{\mathrm{I}e}^T$ is expressible as

$$[\boldsymbol{A}_5]_{mn} = \sum_{p=1}^{N-1} [\boldsymbol{S}_{1e}]_{mp} [\boldsymbol{S}_{\mathrm{I}e}^T]_{pn}, \tag{C17}$$

which after substituting the result of Eq. (C16) becomes

$$[\boldsymbol{A}_5]_{mn} = \sqrt{2N} \sum_{p=1}^{N-1} [\boldsymbol{S}_{\mathrm{I}e}]_{mp} [\boldsymbol{S}_{\mathrm{I}e}^T]_{pn}. \tag{C18}$$

Because the matrix $\boldsymbol{S}_{\mathrm{I}e}$ is unitary, Eq. (C18) can be recast as

$$[\boldsymbol{A}_5]_{mn} = \sqrt{2N}\,\delta(m-n), \tag{C19}$$

from which it is clear that $\boldsymbol{A}_5 = \sqrt{2N}\boldsymbol{I}$.

## Diagonal Relationship for Type-II Even-Length DST

Consider the matrix $\boldsymbol{A}_6 = \boldsymbol{S}_{2e}\boldsymbol{S}_{\mathrm{II}e}^T$. Recall the definitions for the $m-n$th elements of the $N \times N$ type-II even-length DST matrices from Appendix A:

$$[\boldsymbol{S}_{2e}]_{mn} = 2\sin\left(\frac{\pi m(n+\frac{1}{2})}{N}\right), \tag{C20}$$

and

$$[\boldsymbol{S}_{\mathrm{II}e}]_{mn} = \sqrt{\frac{2}{N}k_m}\,\sin\left(\frac{\pi m(n+\frac{1}{2})}{N}\right), \tag{C21}$$

for $m = 1, 2, \ldots, N$ and $n = 0, 1, \ldots, N-1$. The constant, $k_m$, in Eq. (C21) is defined in Eq. (A17). It follows from Eqs. (C20) and (C21) that

$$[\boldsymbol{S}_{2e}]_{mn} = \sqrt{\frac{2N}{k_m}}[\boldsymbol{S}_{\mathrm{II}e}]_{mn}. \tag{C22}$$

The $m-n$th element of the product $\boldsymbol{A}_6 = \boldsymbol{S}_{2e}\boldsymbol{S}_{\mathrm{II}e}^T$ is expressible as

$$[\boldsymbol{A}_6]_{mn} = \sum_{p=0}^{N-1} [\boldsymbol{S}_{2e}]_{mp} [\boldsymbol{S}_{\mathrm{II}e}^T]_{pn}, \tag{C23}$$

which after substituting the result of Eq. (C22) becomes

$$[\boldsymbol{A}_6]_{mn} = \sqrt{\frac{2N}{k_m}} \sum_{p=0}^{N-1} [\boldsymbol{S}_{\mathrm{II}e}]_{mp} [\boldsymbol{S}_{\mathrm{II}e}^T]_{pn}. \tag{C24}$$

Because the matrix $\boldsymbol{S}_{\mathrm{II}e}$ is unitary, Eq. (C24) can be recast as

$$[\boldsymbol{A}_6]_{mn} = \sqrt{\frac{2N}{k_m}} \delta(m-n), \tag{C25}$$

for $m, n = 1, 2, \ldots, N,$ from which $\boldsymbol{A}_6$ is clearly diagonal with the general result for its $m-n$th element given by

$$[\boldsymbol{A}_6]_{mn} = \begin{cases} \sqrt{2N}, & m = n \neq N \\ 2\sqrt{N}, & m = n = N \\ 0, & m \neq n, \end{cases} \tag{C26}$$

or more compactly, $\boldsymbol{A}_6 = \sqrt{\frac{2N}{k_m}} \boldsymbol{I}.$

## Diagonal Relationship for Type-IV Even-Length DST

Consider the matrix $\boldsymbol{A}_8 = \boldsymbol{S}_{4e} \boldsymbol{S}_{\mathrm{IV}e}^T.$ Recall the definitions for the $m-n$th elements of the $N \times N$ type-IV even-length DST matrices from Appendix A:

$$[\boldsymbol{S}_{4e}]_{mn} = 2\sin\left(\frac{\pi(m+\frac{1}{2})(n+\frac{1}{2})}{N}\right), \tag{C27}$$

and

$$[\boldsymbol{S}_{\mathrm{IV}e}]_{mn} = \sqrt{\frac{2}{N}} \sin\left(\frac{\pi(m+\frac{1}{2})(n+\frac{1}{2})}{N}\right), \tag{C28}$$

for $m, n = 0, 1, \ldots, N-1.$ It follows from Eqs. (C27) and (C28) that

$$[\boldsymbol{S}_{4e}]_{mn} = \sqrt{2N} [\boldsymbol{S}_{\mathrm{IV}e}]_{mn}. \tag{C29}$$

The $m-n$th element of the product $\boldsymbol{A}_8 = \boldsymbol{S}_{4e} \boldsymbol{S}_{\mathrm{IV}e}^T$ is expressible as

$$[\boldsymbol{A}_8]_{mn} = \sum_{p=0}^{N-1} [\boldsymbol{S}_{4e}]_{mp} [\boldsymbol{S}_{\mathrm{IV}e}^T]_{pn}, \tag{C30}$$

which after substituting the result of Eq. (C29) becomes

$$[\boldsymbol{A}_8]_{mn} = \sqrt{2N} \sum_{p=0}^{N-1} [\boldsymbol{S}_{\mathrm{IV}e}]_{mp} [\boldsymbol{S}_{\mathrm{IV}e}^T]_{pn}. \tag{C31}$$

Because the matrix $\boldsymbol{S}_{\mathrm{IV}e}$ is unitary, Eq. (C31) can be recast as

$$[\boldsymbol{A}_8]_{mn} = \sqrt{2N}\,\delta(m-n), \tag{C32}$$

from which it is clear that $\boldsymbol{A}_8 = \sqrt{2N}\boldsymbol{I}$.

## Diagonal Relationship for Type-IV Odd-Length DCT

Consider the matrix $\boldsymbol{A}_{12} = \boldsymbol{C}_{4o}\boldsymbol{C}_{\mathrm{IV}o}^T$. Recall the definitions for the $m-n$th elements of the $N-1 \times N-1$ type-IV odd-length DCT matrices from Appendix A:

$$[\boldsymbol{C}_{4o}]_{mn} = 2\cos\left(\frac{2\pi(m+\frac{1}{2})(n+\frac{1}{2})}{2N-1}\right), \tag{C33}$$

and

$$[\boldsymbol{C}_{\mathrm{IV}o}]_{mn} = \frac{2}{\sqrt{2N-1}}\cos\left(\frac{2\pi(m+\frac{1}{2})(n+\frac{1}{2})}{2N-1}\right), \tag{C34}$$

for $m, n = 0, 1, \ldots, N-2$. It follows from Eqs. (C33) and (C34) that

$$[\boldsymbol{C}_{4o}]_{mn} = \sqrt{2N-1}[\boldsymbol{C}_{\mathrm{IV}o}]_{mn}. \tag{C35}$$

The $m-n$th element of the product $\boldsymbol{A}_{12} = \boldsymbol{C}_{4o}\boldsymbol{C}_{\mathrm{IV}o}^T$ is expressible as

$$[\boldsymbol{A}_{12}]_{mn} = \sum_{p=0}^{N-2} [\boldsymbol{C}_{4o}]_{mp} [\boldsymbol{C}_{\mathrm{IV}o}^T]_{pn}, \tag{C36}$$

which after substituting the result of Eq. (C35) becomes

$$[\boldsymbol{A}_{12}]_{mn} = \sqrt{2N-1}\sum_{p=0}^{N-2}[\boldsymbol{C}_{\mathrm{IV}o}]_{mp}[\boldsymbol{C}_{\mathrm{IV}o}^{T}]_{pn}. \tag{C37}$$

Because the matrix $\boldsymbol{C}_{\mathrm{IV}o}$ is unitary, Eq. (C37) can be recast as

$$[\boldsymbol{A}_{12}]_{mn} = \sqrt{2N-1}\,\delta(m-n), \tag{C38}$$

from which it is clear that $\boldsymbol{A}_{12} = \sqrt{2N-1}\boldsymbol{I}$.

## Diagonal Relationship for Type-I Odd-Length DST

Consider the matrix $\boldsymbol{A}_{13} = \boldsymbol{S}_{1o}\boldsymbol{S}_{\mathrm{I}o}^{T}$. Recall the definitions for the $m-n$th elements of the $N-1\times N-1$ type-I odd-length DST matrices from Appendix A:

$$[\boldsymbol{S}_{1o}]_{mn} = 2\sin\left(\frac{2\pi mn}{2N-1}\right), \tag{C39}$$

and

$$[\boldsymbol{S}_{\mathrm{I}o}]_{mn} = \frac{2}{\sqrt{2N-1}}\sin\left(\frac{2\pi mn}{2N-1}\right), \tag{C40}$$

for $m, n = 1, 2, \ldots, N-1$. It follows from Eqs. (C39) and (C40) that

$$[\boldsymbol{S}_{1o}]_{mn} = \sqrt{2N-1}[\boldsymbol{S}_{\mathrm{I}o}]_{mn}. \tag{C41}$$

The $m-n$th element of the product $\boldsymbol{A}_{13} = \boldsymbol{S}_{1o}\boldsymbol{S}_{\mathrm{I}o}^{T}$ is expressible as

$$[\boldsymbol{A}_{13}]_{mn} = \sum_{p=1}^{N-1}[\boldsymbol{S}_{1o}]_{mp}[\boldsymbol{S}_{\mathrm{I}o}^{T}]_{pn}, \tag{C42}$$

which after substituting the result of Eq. (C41) becomes

$$[\boldsymbol{A}_{13}]_{mn} = \sqrt{2N-1}\sum_{p=1}^{N-1}[\boldsymbol{S}_{\mathrm{I}o}]_{mp}[\boldsymbol{S}_{\mathrm{I}o}^{T}]_{pn}. \tag{C43}$$

Because the matrix $\boldsymbol{S}_{\mathrm{I}o}$ is unitary, Eq. (C43) can be recast as

$$[\boldsymbol{A}_{13}]_{mn} = \sqrt{2N-1}\,\delta(m-n), \tag{C44}$$

from which it is clear that $\boldsymbol{A}_{13} = \sqrt{2N-1}\boldsymbol{I}$.

## Diagonal Relationship for Type-II Odd-Length DST

Consider the matrix $\boldsymbol{A}_{14} = \boldsymbol{S}_{2o}\boldsymbol{S}_{\mathrm{II}o}^{T}$. Recall the definitions for the $m-n$th elements of the $N-1 \times N-1$ type-II odd-length DST matrices from Appendix A:

$$[\boldsymbol{S}_{2o}]_{mn} = 2\sin\left(\frac{2\pi m(n+\frac{1}{2})}{2N-1}\right), \tag{C45}$$

and

$$[\boldsymbol{S}_{\mathrm{II}o}]_{mn} = \frac{2}{\sqrt{2N-1}}\sin\left(\frac{2\pi m(n+\frac{1}{2})}{2N-1}\right), \tag{C46}$$

for $m = 1, 2, \ldots, N-1$ and $n = 0, 1, \ldots, N-2$. It follows from Eqs. (C45) and (C46) that

$$[\boldsymbol{S}_{2o}]_{mn} = \sqrt{2N-1}[\boldsymbol{S}_{\mathrm{II}o}]_{mn}. \tag{C47}$$

The $m-n$th element of the product $\boldsymbol{A}_{14} = \boldsymbol{S}_{2o}\boldsymbol{S}_{\mathrm{II}o}^{T}$ is expressible as

$$[\boldsymbol{A}_{14}]_{mn} = \sum_{p=0}^{N-2} [\boldsymbol{S}_{2o}]_{mp}[\boldsymbol{S}_{\mathrm{II}o}^{T}]_{pn}, \tag{C48}$$

which after substituting the result of Eq. (C47) becomes

$$[\boldsymbol{A}_{14}]_{mn} = \sqrt{2N-1}\sum_{p=0}^{N-2} [\boldsymbol{S}_{\mathrm{II}o}]_{mp}[\boldsymbol{S}_{\mathrm{II}o}^{T}]_{pn}. \tag{C49}$$

Because the matrix $\boldsymbol{S}_{\mathrm{II}o}$ is unitary, Eq. (C49) can be recast as

$$[\boldsymbol{A}_{14}]_{mn} = \sqrt{2N-1}\,\delta(m-n), \tag{C50}$$

for $m, n = 1, 2, \ldots, N-1$, from which it is clear that $\boldsymbol{A}_{14} = \sqrt{2N-1}\boldsymbol{I}$.

## Diagonal Relationship for Type-III Odd-Length DST

Consider the matrix $\boldsymbol{A}_{15} = \boldsymbol{S}_{3o}\boldsymbol{S}_{\mathrm{III}o}^{T}$. Recall the definitions for the $m-n$th elements of the $N-1 \times N-1$ type-III odd-length DST matrices from Appendix A:

$$[\boldsymbol{S}_{3o}]_{mn} = 2\sin\left(\frac{2\pi(m+\frac{1}{2})n}{2N-1}\right), \tag{C51}$$

and

$$[\boldsymbol{S}_{\mathrm{III}o}]_{mn} = \frac{2}{\sqrt{2N-1}}\sin\left(\frac{2\pi(m+\frac{1}{2})n}{2N-1}\right), \tag{C52}$$

for $m = 0, 1, \ldots, N-2$ and $n = 1, 2, \ldots, N-1$. It follows from Eqs. (C51) and (C52) that

$$[\boldsymbol{S}_{3o}]_{mn} = \sqrt{2N-1}[\boldsymbol{S}_{\mathrm{III}o}]_{mn}. \tag{C53}$$

Observe that both the convolutional and unitary type-III DSTs are the transposes of type-II DSTs so that $\boldsymbol{S}_{3o} = \boldsymbol{S}_{2o}^{T}$ and $\boldsymbol{S}_{\mathrm{III}o} = \boldsymbol{S}_{\mathrm{II}o}^{T}$. The matrix that relates the convolutional and unitary type-III DSTs can thus be expressed in terms of type-II DSTs as $\boldsymbol{A}_{15} = \boldsymbol{S}_{2o}^{T}\boldsymbol{S}_{\mathrm{II}o}$, or equivalently $\boldsymbol{A}_{15}^{T} = \boldsymbol{S}_{\mathrm{II}o}^{T}\boldsymbol{S}_{2o}$, so that substituting the result of Eq. (C53) produces

$$\begin{aligned} \boldsymbol{A}_{15}^{T} &= \sqrt{2N-1}\boldsymbol{S}_{\mathrm{II}o}^{T}\boldsymbol{S}_{\mathrm{II}o} \\ &= \sqrt{2N-1}\boldsymbol{I}, \end{aligned} \tag{C54}$$

for $m, n = 0, 1, \ldots, N-2$, which is clearly diagonal so that $\boldsymbol{A}_{15} = \sqrt{2N-1}\boldsymbol{I}$.

These nine derivations demonstrate the general diagonal relationships that exist between convolutional and unitary discrete trigonometric transforms (DTTs). Seven DTTs do not have a diagonal relationship in general, which can be easily demonstrated by counterexample.

# Appendix D

# Derivation of Symmetric Convolution Cases Based on Unitary Transform Matrices

This appendix presents derivations of the eighteen cases of symmetric convolution that can be based on unitary transforms. The appendix details each of the forty cases from Appendix B and provides reasons why each case does or does not exist in terms of unitary transform matrices.

## Even-Length Cases

### Case 1

Case 1, $\boldsymbol{d} = \boldsymbol{C}_{1e}^{-1}\boldsymbol{H}_{\boldsymbol{C}_{1e}}\boldsymbol{C}_{1e}\boldsymbol{\theta},$ is not expressible in terms of unitary transform matrices because the matrix $\boldsymbol{A}_1 = \boldsymbol{C}_{1e}\boldsymbol{C}_{1e}^T$ is not, in general, diagonal.

### Case 2

Case 2, which states that

$$\boldsymbol{d} = \boldsymbol{S}_{1e}^{-1}\boldsymbol{H}_{\boldsymbol{C}_{1e}}\boldsymbol{S}_{1e}\boldsymbol{\theta}, \tag{D1}$$

is expressible in terms of unitary transform matrices. The matrix $\boldsymbol{H}_{\boldsymbol{C}_{1e}} = \mathrm{diag}\{\boldsymbol{C}_{1e}\boldsymbol{h}_{WSWS}^r\}$ normally contains $N+1$ samples ranging from 0 to $N$ along its diagonal, but here only the samples from 1 to $N-1$ need to be retained because the underlying symmetry of the vector $\boldsymbol{S}_{1e}\boldsymbol{\theta}$ forces zeros at $m=0$ and $m=N$ which cancel the values of $\boldsymbol{C}_{1e}\boldsymbol{h}^{r}_{WSWS}$ at $m=0$ and $m=N$. Thus each matrix in Eq. (D1) has compatible dimension $N-1\times N-1$. Substituting the fact that $\boldsymbol{S}_{1e}=\boldsymbol{A}_5\boldsymbol{S}_{\mathrm{I}e}$ into Eq. (D1) produces

$$\boldsymbol{d}=\boldsymbol{S}_{\mathrm{I}e}^{-1}\boldsymbol{A}_5^{-1}\boldsymbol{H}_{\boldsymbol{C}_{1e}}\boldsymbol{A}_5\boldsymbol{S}_{\mathrm{I}e}\boldsymbol{\theta}, \tag{D2}$$

where the three interior matrices in Eq. (D2) commute, resulting in

$$\boldsymbol{d}=\boldsymbol{S}_{\mathrm{I}e}^{-1}\boldsymbol{H}_{\boldsymbol{C}_{1e}}\boldsymbol{S}_{\mathrm{I}e}\boldsymbol{\theta}, \tag{D3}$$

which is the desired result based on unitary transform matrices for Case 2.

**Case 3**

Case 3, $\boldsymbol{d}=-\boldsymbol{C}_{1e}^{-1}\boldsymbol{H}_{\boldsymbol{S}_{1e}}\boldsymbol{S}_{1e}\boldsymbol{\theta},$ is not expressible in terms of unitary transform matrices because the matrix $\boldsymbol{A}_1=\boldsymbol{C}_{1e}\boldsymbol{C}_{\mathrm{I}e}^{T}$ is not, in general, diagonal.

**Case 4**

Case 4, which states that

$$\boldsymbol{d}=\boldsymbol{C}_{2e}^{-1}\boldsymbol{H}_{\boldsymbol{C}_{1e}}\boldsymbol{C}_{2e}\boldsymbol{\theta}, \tag{D4}$$

is expressible in terms of unitary transform matrices. The matrix $\boldsymbol{H}_{\boldsymbol{C}_{1e}}=\mathrm{diag}\{\boldsymbol{C}_{1e}\boldsymbol{h}^{r}_{WSWS}\}$ normally contains $N+1$ samples ranging from 0 to $N$ along its diagonal, but here only the first $N$ samples from 0 to $N-1$ need to be retained because the underlying symmetry of the vector $\boldsymbol{C}_{2e}\boldsymbol{\theta}$ forces a zero at $m=N$ which cancels the value of $\boldsymbol{C}_{1e}\boldsymbol{h}^{r}_{WSWS}$ at $m=N$. Thus each matrix in Eq. (D4) has compatible dimension $N\times N$. Substituting the fact that $\boldsymbol{C}_{2e}=\boldsymbol{A}_2\boldsymbol{C}_{\mathrm{II}e}$ into Eq. (D4) produces

$$\boldsymbol{d}=\boldsymbol{C}_{\mathrm{II}e}^{-1}\boldsymbol{A}_2^{-1}\boldsymbol{H}_{\boldsymbol{C}_{1e}}\boldsymbol{A}_2\boldsymbol{C}_{\mathrm{II}e}\boldsymbol{\theta}, \tag{D5}$$

where the three interior matrices in Eq. (D5) commute, resulting in

$$\boldsymbol{d} = \boldsymbol{C}_{\mathrm{II}e}^{-1} \boldsymbol{H}_{\boldsymbol{C}_{1e}} \boldsymbol{C}_{\mathrm{II}e} \boldsymbol{\theta}, \tag{D6}$$

which is the desired result based on unitary transform matrices for Case 4.

**Case 5**

Case 5, which states that

$$\boldsymbol{d} = \boldsymbol{S}_{2e}^{-1} \boldsymbol{H}_{\boldsymbol{S}_{1e}} \boldsymbol{C}_{2e} \boldsymbol{\theta}, \tag{D7}$$

is expressible in terms of unitary transform matrices. The matrix $\boldsymbol{H}_{\boldsymbol{S}_{1e}} = \mathrm{diag}\{\boldsymbol{S}_{1e} \boldsymbol{h}_{WAWA}^{r}\}$ contains $N-1$ samples ranging from 1 to $N-1$ along its diagonal, so that only the last $N-1$ samples of the vector $\boldsymbol{C}_{2e}\boldsymbol{\theta}$ from 1 to $N-1$ need to be retained because the underlying symmetry of the vector $\boldsymbol{S}_{1e} \boldsymbol{h}_{WAWA}^{r}$ forces a zero at $m = 0$ which cancels the values of the vector $\boldsymbol{C}_{2e}\boldsymbol{\theta}$ at $m = 0$. Thus each matrix in Eq. (D7) has compatible dimension $N-1 \times N-1$. Substituting the facts that $\boldsymbol{S}_{2e} = \boldsymbol{A}_6 \boldsymbol{S}_{\mathrm{II}e}$ and $\boldsymbol{C}_{2e} = \boldsymbol{A}_2 \boldsymbol{C}_{\mathrm{II}e}$ into Eq. (D7) produces

$$\boldsymbol{d} = \boldsymbol{S}_{\mathrm{II}e}^{-1} \boldsymbol{A}_6^{-1} \boldsymbol{H}_{\boldsymbol{S}_{1e}} \boldsymbol{A}_2 \boldsymbol{C}_{\mathrm{II}e} \boldsymbol{\theta}, \tag{D8}$$

where the three interior matrices in Eq. (D8) commute, resulting in

$$\boldsymbol{d} = \boldsymbol{S}_{\mathrm{II}e}^{-1} \boldsymbol{H}_{\boldsymbol{S}_{1e}} \boldsymbol{C}_{\mathrm{II}e} \boldsymbol{\theta}, \tag{D9}$$

because the matrices $\boldsymbol{A}_2$ and $\boldsymbol{A}_6$ are identical over index values of 1 to $N-1$, and which is the desired result based on unitary transform matrices for Case 5.

**Case 6**

Case 6, which states that

$$\boldsymbol{d} = \boldsymbol{S}_{2e}^{-1} \boldsymbol{H}_{\boldsymbol{C}_{1e}} \boldsymbol{S}_{2e} \boldsymbol{\theta}, \tag{D10}$$

is expressible in terms of unitary transform matrices. The matrix $\boldsymbol{H}_{\boldsymbol{C}_{1e}} = \mathrm{diag}\{\boldsymbol{C}_{1e}\boldsymbol{h}^{r}_{WSWS}\}$ normally contains $N+1$ samples ranging from 0 to $N$ along its diagonal, but here only the last $N$ samples from 1 to $N$ need to be retained because the underlying symmetry of the vector $\boldsymbol{S}_{2e}\boldsymbol{\theta}$ forces a zero at $m=0$ which cancels the value of $\boldsymbol{C}_{1e}\boldsymbol{h}^{r}_{WSWS}$ at $m=0$. Thus each matrix in Eq. (D10) has compatible dimension $N \times N$. Substituting the fact that $\boldsymbol{S}_{2e} = \boldsymbol{A}_6\boldsymbol{S}_{\mathrm{II}e}$ into Eq. (D10) produces

$$\boldsymbol{d} = \boldsymbol{S}^{-1}_{\mathrm{II}e}\boldsymbol{A}^{-1}_{6}\boldsymbol{H}_{\boldsymbol{C}_{1e}}\boldsymbol{A}_6\boldsymbol{S}_{\mathrm{II}e}\boldsymbol{\theta}, \tag{D11}$$

where the three interior matrices in Eq. (D11) commute, resulting in

$$\boldsymbol{d} = \boldsymbol{S}^{-1}_{\mathrm{II}e}\boldsymbol{H}_{\boldsymbol{C}_{1e}}\boldsymbol{S}_{\mathrm{II}e}\boldsymbol{\theta}, \tag{D12}$$

which is the desired result based on unitary transform matrices for Case 6.

**Case 7**

Case 7, which states that

$$\boldsymbol{d} = -\boldsymbol{C}^{-1}_{2e}\boldsymbol{H}_{\boldsymbol{S}_{1e}}\boldsymbol{S}_{2e}\boldsymbol{\theta}, \tag{D13}$$

is expressible in terms of unitary transform matrices. The matrix $\boldsymbol{H}_{\boldsymbol{S}_{1e}} = \mathrm{diag}\{\boldsymbol{S}_{1e}\boldsymbol{h}^{r}_{WAWA}\}$ contains $N-1$ samples ranging from 1 to $N-1$ along its diagonal, so that only the first $N-1$ samples of the vector $\boldsymbol{S}_{2e}\boldsymbol{\theta}$ from 1 to $N-1$ need to be retained because the underlying symmetry of the vector $\boldsymbol{S}_{1e}\boldsymbol{h}^{r}_{WAWA}$ forces a zero at $m=N$ which cancels the values of the vector $\boldsymbol{S}_{2e}\boldsymbol{\theta}$ at $m=N$. Thus each matrix in Eq. (D13) has compatible dimension $N-1 \times N-1$. Substituting the facts that $\boldsymbol{C}_{2e} = \boldsymbol{A}_2\boldsymbol{C}_{\mathrm{II}e}$ and $\boldsymbol{S}_{2e} = \boldsymbol{A}_6\boldsymbol{S}_{\mathrm{II}e}$ into Eq. (D13) produces

$$\boldsymbol{d} = -\boldsymbol{C}^{-1}_{\mathrm{II}e}\boldsymbol{A}^{-1}_{2}\boldsymbol{H}_{\boldsymbol{S}_{1e}}\boldsymbol{A}_6\boldsymbol{S}_{\mathrm{II}e}\boldsymbol{\theta}, \tag{D14}$$

where the three interior matrices in Eq. (D14) commute, resulting in

$$\boldsymbol{d} = -\boldsymbol{C}_{\mathrm{II}e}^{-1}\boldsymbol{H}_{\boldsymbol{S}_{1e}}\boldsymbol{S}_{\mathrm{II}e}\boldsymbol{\theta}, \tag{D15}$$

because the matrices $\boldsymbol{A}_2$ and $\boldsymbol{A}_6$ are identical over index values of 1 to $N-1$, and which is the desired result based on unitary transform matrices for Case 7.

**Case 8**

Case 8, $\boldsymbol{d} = \boldsymbol{C}_{1e}^{-1}\boldsymbol{H}_{\boldsymbol{C}_{2e}}\boldsymbol{C}_{2e}\boldsymbol{\theta}$, is not expressible in terms of unitary transform matrices because the matrix $\boldsymbol{A}_1 = \boldsymbol{C}_{1e}\boldsymbol{C}_{\mathrm{I}e}^T$ is not, in general, diagonal.

**Case 9**

Case 9, which states that

$$\boldsymbol{d} = \boldsymbol{S}_{1e}^{-1}\boldsymbol{H}_{\boldsymbol{S}_{2e}}\boldsymbol{C}_{2e}\boldsymbol{\theta}, \tag{D16}$$

is expressible in terms of unitary transform matrices. The matrix $\boldsymbol{H}_{\boldsymbol{S}_{2e}} = \mathrm{diag}\{\boldsymbol{S}_{2e}\boldsymbol{h}_{HAHA}^r\}$ contains $N$ samples ranging from 1 to $N$ along its diagonal, so that only the last $N-1$ samples of the vector $\boldsymbol{C}_{2e}\boldsymbol{\theta}$ from 1 to $N-1$ need to be retained because the underlying symmetry of the vector $\boldsymbol{S}_{2e}\boldsymbol{h}_{HAHA}^r$ forces a zero at $m=0$ which cancels the values of the vector $\boldsymbol{C}_{2e}\boldsymbol{\theta}$ at $m=0$. Thus each matrix in Eq. (D16) has compatible dimension $N-1\times N-1$. Substituting the facts that $\boldsymbol{S}_{1e} = \boldsymbol{A}_5\boldsymbol{S}_{\mathrm{I}e}$ and $\boldsymbol{C}_{2e} = \boldsymbol{A}_2\boldsymbol{C}_{\mathrm{II}e}$ into Eq. (D16) produces

$$\boldsymbol{d} = \boldsymbol{S}_{\mathrm{I}e}^{-1}\boldsymbol{A}_5^{-1}\boldsymbol{H}_{\boldsymbol{S}_{2e}}\boldsymbol{A}_2\boldsymbol{C}_{\mathrm{II}e}\boldsymbol{\theta}, \tag{D17}$$

where the three interior matrices in Eq. (D17) commute, resulting in

$$\boldsymbol{d} = \boldsymbol{S}_{\mathrm{I}e}^{-1}\boldsymbol{H}_{\boldsymbol{S}_{2e}}\boldsymbol{C}_{\mathrm{II}e}\boldsymbol{\theta}, \tag{D18}$$

because the matrices $\boldsymbol{A}_2$ and $\boldsymbol{A}_5$ are identical over index values of 1 to $N-1$, and which is the desired result based on unitary transform matrices for Case 9.

**Case 10**

Case 10, $\boldsymbol{d} = -\boldsymbol{C}_{1e}^{-1}\boldsymbol{H}_{\boldsymbol{S}_{2e}}\boldsymbol{S}_{2e}\boldsymbol{\theta}$, is not expressible in terms of unitary transform matrices because the matrix $\boldsymbol{A}_1 = \boldsymbol{C}_{1e}\boldsymbol{C}_{\mathrm{I}e}^T$ is not, in general, diagonal.

**Case 11**

Case 11, $\boldsymbol{d} = \boldsymbol{C}_{3e}^{-1}\boldsymbol{H}_{\boldsymbol{C}_{3e}}\boldsymbol{C}_{3e}\boldsymbol{\theta}$, is not expressible in terms of unitary transform matrices because the matrix $\boldsymbol{A}_3 = \boldsymbol{C}_{3e}\boldsymbol{C}_{\mathrm{III}e}^T$ is not, in general, diagonal.

**Case 12**

Case 12, $\boldsymbol{d} = \boldsymbol{S}_{3e}^{-1}\boldsymbol{H}_{\boldsymbol{C}_{3e}}\boldsymbol{S}_{3e}\boldsymbol{\theta}$, is not expressible in terms of unitary transform matrices because the matrices $\boldsymbol{A}_3 = \boldsymbol{C}_{3e}\boldsymbol{C}_{\mathrm{III}e}^T$ and $\boldsymbol{A}_7 = \boldsymbol{S}_{3e}\boldsymbol{S}_{\mathrm{III}e}^T$ are not, in general, diagonal.

**Case 13**

Case 13, $\boldsymbol{d} = -\boldsymbol{C}_{3e}^{-1}\boldsymbol{H}_{\boldsymbol{S}_{3e}}\boldsymbol{S}_{3e}\boldsymbol{\theta}$, is not expressible in terms of unitary transform matrices because the matrices $\boldsymbol{A}_3 = \boldsymbol{C}_{3e}\boldsymbol{C}_{\mathrm{III}e}^T$ and $\boldsymbol{A}_7 = \boldsymbol{S}_{3e}\boldsymbol{S}_{\mathrm{III}e}^T$ are not, in general, diagonal.

**Case 14**

Case 14, which states that

$$\boldsymbol{d} = \boldsymbol{C}_{4e}^{-1}\boldsymbol{H}_{\boldsymbol{C}_{3e}}\boldsymbol{C}_{4e}\boldsymbol{\theta}, \tag{D19}$$

is expressible in terms of unitary transform matrices. The matrix $\boldsymbol{H}_{\boldsymbol{C}_{3e}} = \mathrm{diag}\left\{\boldsymbol{C}_{3e}\boldsymbol{h}_{WSWA}^r\right\}$ contains $N$ samples ranging from 0 to $N-1$ along its diagonal, so that each matrix in

Eq. (D19) has compatible dimension $N \times N$. Substituting the fact that $\boldsymbol{C}_{4e} = \boldsymbol{A}_4 \boldsymbol{C}_{\mathrm{IV}e}$ into Eq. (D19) produces

$$\boldsymbol{d} = \boldsymbol{C}_{\mathrm{IV}e}^{-1} \boldsymbol{A}_4^{-1} \boldsymbol{H}_{\boldsymbol{C}_{3e}} \boldsymbol{A}_4 \boldsymbol{C}_{\mathrm{IV}e} \boldsymbol{\theta}, \tag{D20}$$

where the three interior matrices in Eq. (D20) commute, resulting in

$$\boldsymbol{d} = \boldsymbol{C}_{\mathrm{IV}e}^{-1} \boldsymbol{H}_{\boldsymbol{C}_{3e}} \boldsymbol{C}_{\mathrm{IV}e} \boldsymbol{\theta}, \tag{D21}$$

which is the desired result based on unitary transform matrices for Case 14.

**Case 15**

Case 15, which states that

$$\boldsymbol{d} = \boldsymbol{S}_{4e}^{-1} \boldsymbol{H}_{\boldsymbol{S}_{3e}} \boldsymbol{C}_{4e} \boldsymbol{\theta}, \tag{D22}$$

is expressible in terms of unitary transform matrices. The matrix $\boldsymbol{H}_{\boldsymbol{S}_{3e}} = \mathrm{diag}\{\boldsymbol{S}_{3e} \boldsymbol{h}_{WAWS}^{r}\}$ contains $N$ samples ranging from 0 to $N-1$ along its diagonal, so that each matrix in Eq. (D22) has compatible dimension $N \times N$. Substituting the facts that $\boldsymbol{S}_{4e} = \boldsymbol{A}_8 \boldsymbol{S}_{\mathrm{IV}e}$ and $\boldsymbol{C}_{4e} = \boldsymbol{A}_4 \boldsymbol{C}_{\mathrm{IV}e}$ into Eq. (D22) produces

$$\boldsymbol{d} = \boldsymbol{S}_{\mathrm{IV}e}^{-1} \boldsymbol{A}_8^{-1} \boldsymbol{H}_{\boldsymbol{S}_{3e}} \boldsymbol{A}_4 \boldsymbol{C}_{\mathrm{IV}e} \boldsymbol{\theta}, \tag{D23}$$

where the three interior matrices in Eq. (D23) commute, resulting in

$$\boldsymbol{d} = \boldsymbol{S}_{\mathrm{IV}e}^{-1} \boldsymbol{H}_{\boldsymbol{S}_{3e}} \boldsymbol{C}_{\mathrm{IV}e} \boldsymbol{\theta}, \tag{D24}$$

because the matrices $\boldsymbol{A}_4$ and $\boldsymbol{A}_8$ are identical, and which is the desired result based on unitary transform matrices for Case 15.

**Case 16**

Case 16, which states that

$$\boldsymbol{d} = \boldsymbol{S}_{4e}^{-1} \boldsymbol{H}_{\boldsymbol{C}_{3e}} \boldsymbol{S}_{4e} \boldsymbol{\theta}, \tag{D25}$$

is expressible in terms of unitary transform matrices. The matrix $\boldsymbol{H}_{\boldsymbol{C}_{3e}} = \operatorname{diag}\{\boldsymbol{C}_{3e}\boldsymbol{h}_{WSWA}^{r}\}$ contains $N$ samples ranging from 0 to $N-1$ along its diagonal, so that each matrix in Eq. (D25) has compatible dimension $N \times N$. Substituting the fact that $\boldsymbol{S}_{4e} = \boldsymbol{A}_8\boldsymbol{S}_{\mathrm{IV}e}$ into Eq. (D25) produces

$$\boldsymbol{d} = \boldsymbol{S}_{\mathrm{IV}e}^{-1}\boldsymbol{A}_8^{-1}\boldsymbol{H}_{\boldsymbol{C}_{3e}}\boldsymbol{A}_8\boldsymbol{S}_{\mathrm{IV}e}\boldsymbol{\theta}, \tag{D26}$$

where the three interior matrices in Eq. (D26) commute, resulting in

$$\boldsymbol{d} = \boldsymbol{S}_{\mathrm{IV}e}^{-1}\boldsymbol{H}_{\boldsymbol{C}_{3e}}\boldsymbol{S}_{\mathrm{IV}e}\boldsymbol{\theta}, \tag{D27}$$

which is the desired result based on unitary transform matrices for Case 16.

**Case 17**

Case 17, which states that

$$\boldsymbol{d} = -\boldsymbol{C}_{4e}^{-1}\boldsymbol{H}_{\boldsymbol{S}_{3e}}\boldsymbol{S}_{4e}\boldsymbol{\theta} \tag{D28}$$

is expressible in terms of unitary transform matrices. The matrix $\boldsymbol{H}_{\boldsymbol{S}_{3e}} = \operatorname{diag}\{\boldsymbol{S}_{3e}\boldsymbol{h}_{WAWS}^{r}\}$ contains $N$ samples ranging from 0 to $N-1$ along its diagonal, so that each matrix in Eq. (D28) has compatible dimension $N \times N$. Substituting the facts that $\boldsymbol{C}_{4e} = \boldsymbol{A}_4\boldsymbol{C}_{\mathrm{IV}e}$ and $\boldsymbol{S}_{4e} = \boldsymbol{A}_8\boldsymbol{S}_{\mathrm{IV}e}$ into Eq. (D28) produces

$$\boldsymbol{d} = -\boldsymbol{C}_{\mathrm{IV}e}^{-1}\boldsymbol{A}_4^{-1}\boldsymbol{H}_{\boldsymbol{S}_{3e}}\boldsymbol{A}_8\boldsymbol{S}_{\mathrm{IV}e}\boldsymbol{\theta}, \tag{D29}$$

where the three interior matrices in Eq. (D29) commute, resulting in

$$\boldsymbol{d} = -\boldsymbol{C}_{\mathrm{IV}e}^{-1}\boldsymbol{H}_{\boldsymbol{S}_{3e}}\boldsymbol{S}_{\mathrm{IV}e}\boldsymbol{\theta}, \tag{D30}$$

because the matrices $\boldsymbol{A}_4$ and $\boldsymbol{A}_8$ are identical, and which is the desired result based on unitary transform matrices for Case 17.

**Case 18**

Case 18, $\boldsymbol{d} = \boldsymbol{C}_{3e}^{-1}\boldsymbol{H}_{\boldsymbol{C}_{4e}}\boldsymbol{C}_{4e}\boldsymbol{\theta}$, is not expressible in terms of unitary transform matrices because the matrix $\boldsymbol{A}_3 = \boldsymbol{C}_{3e}\boldsymbol{C}_{\mathrm{III}e}^T$ is not, in general, diagonal.

**Case 19**

Case 19, $\boldsymbol{d} = \boldsymbol{S}_{3e}^{-1}\boldsymbol{H}_{\boldsymbol{S}_{4e}}\boldsymbol{C}_{4e}\boldsymbol{\theta}$, is not expressible in terms of unitary transform matrices because the matrix $\boldsymbol{A}_7 = \boldsymbol{S}_{3e}\boldsymbol{S}_{\mathrm{III}e}^T$ is not, in general, diagonal.

**Case 20**

Case 20, $\boldsymbol{d} = -\boldsymbol{C}_{3e}^{-1}\boldsymbol{H}_{\boldsymbol{S}_{4e}}\boldsymbol{S}_{4e}\boldsymbol{\theta}$, is not expressible in terms of unitary transform matrices because the matrix $\boldsymbol{A}_3 = \boldsymbol{C}_{3e}\boldsymbol{C}_{\mathrm{III}e}^T$ is not, in general, diagonal.

## Odd-Length Cases

**Case 21**

Case 21, $\boldsymbol{d} = \boldsymbol{C}_{1o}^{-1}\boldsymbol{H}_{\boldsymbol{C}_{1o}}\boldsymbol{C}_{1o}\boldsymbol{\theta}$, is not expressible in terms of unitary transform matrices because the matrix $\boldsymbol{A}_9 = \boldsymbol{C}_{1o}\boldsymbol{C}_{\mathrm{I}o}^T$ is not, in general, diagonal.

**Case 22**

Case 22, which states that

$$\boldsymbol{d} = \boldsymbol{S}_{1o}^{-1}\boldsymbol{H}_{\boldsymbol{C}_{1o}}\boldsymbol{S}_{1o}\boldsymbol{\theta}, \tag{D31}$$

is expressible in terms of unitary transform matrices. The matrix $\boldsymbol{H}_{\boldsymbol{C}_{1o}} = \mathrm{diag}\{\boldsymbol{C}_{1o}\boldsymbol{h}_{WSHS}^r\}$ normally contains $N$ samples ranging from 0 to $N-1$ along its diagonal, but here only the samples from 1 to $N-1$ need to be retained because the underlying symmetry of the vector $\boldsymbol{S}_{1o}\boldsymbol{\theta}$ forces a zero at $m = 0$ which cancels the value of $\boldsymbol{C}_{1o}\boldsymbol{h}^{r}_{WSHS}$ at $m = 0$. Thus each matrix in Eq. (D31) has compatible dimension $N-1\times N-1$. Substituting the fact that $\boldsymbol{S}_{1o} = \boldsymbol{A}_{13}\boldsymbol{S}_{\mathrm{I}o}$ into Eq. (D31) produces

$$\boldsymbol{d} = \boldsymbol{S}_{\mathrm{I}o}^{-1}\boldsymbol{A}_{13}^{-1}\boldsymbol{H}_{\boldsymbol{C}_{1o}}\boldsymbol{A}_{13}\boldsymbol{S}_{\mathrm{I}o}\boldsymbol{\theta}, \qquad \text{(D32)}$$

where the three interior matrices in Eq. (D32) commute, resulting in

$$\boldsymbol{d} = \boldsymbol{S}_{\mathrm{I}o}^{-1}\boldsymbol{H}_{\boldsymbol{C}_{1o}}\boldsymbol{S}_{\mathrm{I}o}\boldsymbol{\theta}, \qquad \text{(D33)}$$

which is the desired result based on unitary transform matrices for Case 22.

**Case 23**

Case 23, $\boldsymbol{d} = -\boldsymbol{C}_{1o}^{-1}\boldsymbol{H}_{\boldsymbol{S}_{1o}}\boldsymbol{S}_{1o}\boldsymbol{\theta}$, is not expressible in terms of unitary transform matrices because the matrix $\boldsymbol{A}_9 = \boldsymbol{C}_{1o}\boldsymbol{C}_{\mathrm{I}o}^{T}$ is not, in general, diagonal.

**Case 24**

Case 24, $\boldsymbol{d} = \boldsymbol{C}_{2o}^{-1}\boldsymbol{H}_{\boldsymbol{C}_{2o}}\boldsymbol{C}_{1o}\boldsymbol{\theta}$, is not expressible in terms of unitary transform matrices because the matrices $\boldsymbol{A}_9 = \boldsymbol{C}_{1o}\boldsymbol{C}_{\mathrm{I}o}^{T}$ and $\boldsymbol{A}_{10} = \boldsymbol{C}_{2o}\boldsymbol{C}_{\mathrm{II}o}^{T}$ are not, in general, diagonal.

**Case 25**

Case 25, which states that

$$\boldsymbol{d} = \boldsymbol{S}_{2o}^{-1}\boldsymbol{H}_{\boldsymbol{C}_{2o}}\boldsymbol{S}_{1o}\boldsymbol{\theta}, \qquad \text{(D34)}$$

is expressible in terms of unitary transform matrices. The matrix $\boldsymbol{H}_{\boldsymbol{C}_{2o}} = \mathrm{diag}\left\{\boldsymbol{C}_{2o}\boldsymbol{h}^{r}_{HSWS}\right\}$ normally contains $N$ samples ranging from 0 to $N-1$ along its diagonal, but here only the samples from 1 to $N-1$ need to be retained because the underlying symmetry of the vector $\boldsymbol{S}_{1o}\boldsymbol{\theta}$ forces a zero at $m = 0$ which cancels the value of $\boldsymbol{C}_{2o}\boldsymbol{h}^{r}_{HSWS}$ at $m = 0$. Thus each matrix in Eq. (D34) has compatible dimension $N-1\times N-1$. Substituting the facts that $\boldsymbol{S}_{2o}=\boldsymbol{A}_{14}\boldsymbol{S}_{\mathrm{II}o}$ and $\boldsymbol{S}_{1o}=\boldsymbol{A}_{13}\boldsymbol{S}_{\mathrm{I}o}$ into Eq. (D34) produces

$$\boldsymbol{d}=\boldsymbol{S}_{\mathrm{II}o}^{-1}\boldsymbol{A}_{14}^{-1}\boldsymbol{H}_{\boldsymbol{C}_{2o}}\boldsymbol{A}_{13}\boldsymbol{S}_{\mathrm{I}o}\boldsymbol{\theta}, \tag{D35}$$

where the three interior matrices in Eq. (D35) commute, resulting in

$$\boldsymbol{d}=\boldsymbol{S}_{\mathrm{II}o}^{-1}\boldsymbol{H}_{\boldsymbol{C}_{2o}}\boldsymbol{S}_{\mathrm{I}o}\boldsymbol{\theta}, \tag{D36}$$

because the matrices $\boldsymbol{A}_{13}$ and $\boldsymbol{A}_{14}$ are identical, and which is the desired result based on unitary transform matrices for Case 25.

**Case 26**

Case 26, which states that

$$\boldsymbol{d}=\boldsymbol{S}_{2o}^{-1}\boldsymbol{H}_{\boldsymbol{C}_{1o}}\boldsymbol{S}_{2o}\boldsymbol{\theta}, \tag{D37}$$

is expressible in terms of unitary transform matrices. The matrix $\boldsymbol{H}_{\boldsymbol{C}_{1o}}=\mathrm{diag}\{\boldsymbol{C}_{1o}\boldsymbol{h}_{WSHS}^{r}\}$ normally contains $N$ samples ranging from 0 to $N-1$ along its diagonal, but here only the samples from 1 to $N-1$ need to be retained because the underlying symmetry of the vector $\boldsymbol{S}_{2o}\boldsymbol{\theta}$ forces a zero at $m=0$ which cancels the value of $\boldsymbol{C}_{1o}\boldsymbol{h}_{WSHS}^{r}$ at $m=0$. Thus each matrix in Eq. (D37) has compatible dimension $N-1\times N-1$. Substituting the fact that $\boldsymbol{S}_{2o}=\boldsymbol{A}_{14}\boldsymbol{S}_{\mathrm{II}o}$ into Eq. (D37) produces

$$\boldsymbol{d}=\boldsymbol{S}_{\mathrm{II}o}^{-1}\boldsymbol{A}_{14}^{-1}\boldsymbol{H}_{\boldsymbol{C}_{1o}}\boldsymbol{A}_{14}\boldsymbol{S}_{\mathrm{II}o}\boldsymbol{\theta}, \tag{D38}$$

where the three interior matrices in Eq. (D38) commute, resulting in

$$\boldsymbol{d}=\boldsymbol{S}_{\mathrm{II}o}^{-1}\boldsymbol{H}_{\boldsymbol{C}_{1o}}\boldsymbol{S}_{\mathrm{II}o}\boldsymbol{\theta}, \tag{D39}$$

which is the desired result based on unitary transform matrices for Case 26.

**Case 27**

Case 27, $\boldsymbol{d} = -\boldsymbol{C}_{2o}^{-1}\boldsymbol{H}_{\boldsymbol{S}_{1o}}\boldsymbol{S}_{2o}\boldsymbol{\theta}$, is not expressible in terms of unitary transform matrices because the matrix $\boldsymbol{A}_{10} = \boldsymbol{C}_{2o}\boldsymbol{C}_{\mathrm{II}o}^{T}$ is not, in general, diagonal.

**Case 28**

Case 28, $\boldsymbol{d} = \boldsymbol{C}_{1o}^{-1}\boldsymbol{H}_{\boldsymbol{C}_{2o}}\boldsymbol{C}_{2o}\boldsymbol{\theta}$, is not expressible in terms of unitary transform matrices because the matrices $\boldsymbol{A}_{9} = \boldsymbol{C}_{1o}\boldsymbol{C}_{\mathrm{I}o}^{T}$ and $\boldsymbol{A}_{10} = \boldsymbol{C}_{2o}\boldsymbol{C}_{\mathrm{II}o}^{T}$ are not, in general, diagonal.

**Case 29**

Case 29, which states that

$$\boldsymbol{d} = \boldsymbol{S}_{1o}^{-1}\boldsymbol{H}_{\boldsymbol{C}_{2o}}\boldsymbol{S}_{2o}\boldsymbol{\theta}, \tag{D40}$$

is expressible in terms of unitary transform matrices. The matrix $\boldsymbol{H}_{\boldsymbol{C}_{2o}} = \mathrm{diag}\{\boldsymbol{C}_{2o}\boldsymbol{h}_{HSWS}^{r}\}$ normally contains $N$ samples ranging from 0 to $N-1$ along its diagonal, but here only the samples from 1 to $N-1$ need to be retained because the underlying symmetry of the vector $\boldsymbol{S}_{2o}\boldsymbol{\theta}$ forces a zero at $m=0$ which cancels the value of $\boldsymbol{C}_{2o}\boldsymbol{h}_{HSWS}^{r}$ at $m=0$. Thus each matrix in Eq. (D40) has compatible dimension $N-1\times N-1$. Substituting the facts that $\boldsymbol{S}_{1o} = \boldsymbol{A}_{13}\boldsymbol{S}_{\mathrm{I}o}$ and $\boldsymbol{S}_{2o} = \boldsymbol{A}_{14}\boldsymbol{S}_{\mathrm{II}o}$ into Eq. (D40) produces

$$\boldsymbol{d} = \boldsymbol{S}_{\mathrm{I}o}^{-1}\boldsymbol{A}_{13}^{-1}\boldsymbol{H}_{\boldsymbol{C}_{2o}}\boldsymbol{A}_{14}\boldsymbol{S}_{\mathrm{II}o}\boldsymbol{\theta}, \tag{D41}$$

where the three interior matrices in Eq. (D41) commute, resulting in

$$\boldsymbol{d} = \boldsymbol{S}_{\mathrm{I}o}^{-1}\boldsymbol{H}_{\boldsymbol{C}_{2o}}\boldsymbol{S}_{\mathrm{II}o}\boldsymbol{\theta}, \tag{D42}$$

because the matrices $\boldsymbol{A}_{13}$ and $\boldsymbol{A}_{14}$ are identical, and which is the desired result based on unitary transform matrices for Case 29.

**Case 30**

Case 30, $\boldsymbol{d} = -\boldsymbol{C}_{1o}^{-1}\boldsymbol{H}_{\boldsymbol{S}_{2o}}\boldsymbol{S}_{2o}\boldsymbol{\theta}$, is not expressible in terms of unitary transform matrices because the matrix $\boldsymbol{A}_9 = \boldsymbol{C}_{1o}\boldsymbol{C}_{\mathrm{I}o}^T$ is not, in general, diagonal.

**Case 31**

Case 31, $\boldsymbol{d} = \boldsymbol{C}_{3o}^{-1}\boldsymbol{H}_{\boldsymbol{C}_{3o}}\boldsymbol{C}_{3o}\boldsymbol{\theta}$, is not expressible in terms of unitary transform matrices because the matrix $\boldsymbol{A}_{11} = \boldsymbol{C}_{3o}\boldsymbol{C}_{\mathrm{III}o}^T$ is not, in general, diagonal.

**Case 32**

Case 32, which states that

$$\boldsymbol{d} = \boldsymbol{S}_{3o}^{-1}\boldsymbol{H}_{\boldsymbol{C}_{3o}}\boldsymbol{S}_{3o}\boldsymbol{\theta}, \tag{D43}$$

is expressible in terms of unitary transform matrices. The matrix $\boldsymbol{H}_{\boldsymbol{C}_{3o}} = \mathrm{diag}\{\boldsymbol{C}_{3o}\boldsymbol{h}_{WSHA}^r\}$ normally contains $N$ samples ranging from 0 to $N-1$ along its diagonal, but here only the samples from 0 to $N-2$ need to be retained because the underlying symmetry of the vector $\boldsymbol{S}_{3o}\boldsymbol{\theta}$ forces a zero at $m = N-1$ which cancels the value of $\boldsymbol{C}_{3o}\boldsymbol{h}_{WSHA}^r$ at $m = N-1$. Thus each matrix in Eq. (D43) has compatible dimension $N-1\times N-1$. Substituting the fact that $\boldsymbol{S}_{3o} = \boldsymbol{A}_{15}\boldsymbol{S}_{\mathrm{III}o}$ into Eq. (D43) produces

$$\boldsymbol{d} = \boldsymbol{S}_{\mathrm{III}o}^{-1}\boldsymbol{A}_{15}^{-1}\boldsymbol{H}_{\boldsymbol{C}_{3o}}\boldsymbol{A}_{15}\boldsymbol{S}_{\mathrm{III}o}\boldsymbol{\theta}, \tag{D44}$$

where the three interior matrices in Eq. (D44) commute, resulting in

$$\boldsymbol{d} = \boldsymbol{S}_{\mathrm{III}o}^{-1}\boldsymbol{H}_{\boldsymbol{C}_{3o}}\boldsymbol{S}_{\mathrm{III}o}\boldsymbol{\theta}, \tag{D45}$$

which is the desired result based on unitary transform matrices for Case 32.

**Case 33**

Case 33, $\boldsymbol{d} = -\boldsymbol{C}_{3o}^{-1}\boldsymbol{H}_{\boldsymbol{S}_{3o}}\boldsymbol{S}_{3o}\boldsymbol{\theta}$, is not expressible in terms of unitary transform matrices because the matrix $\boldsymbol{A}_{11} = \boldsymbol{C}_{3o}\boldsymbol{C}_{\mathrm{III}o}^{T}$ is not, in general, diagonal.

**Case 34**

Case 34, which states that

$$\boldsymbol{d} = \boldsymbol{C}_{4o}^{-1}\boldsymbol{H}_{\boldsymbol{C}_{3o}}\boldsymbol{C}_{4o}\boldsymbol{\theta}, \tag{D46}$$

is expressible in terms of unitary transform matrices. The matrix $\boldsymbol{H}_{\boldsymbol{C}_{3o}} = \mathrm{diag}\left\{\boldsymbol{C}_{3o}\boldsymbol{h}_{WSHA}^{r}\right\}$ normally contains $N$ samples ranging from 0 to $N-1$ along its diagonal, but here only the samples from 0 to $N-2$ need to be retained because the underlying symmetry of the vector $\boldsymbol{C}_{4o}\boldsymbol{\theta}$ forces a zero at $m = N-1$ which cancels the value of $\boldsymbol{C}_{3o}\boldsymbol{h}_{WSHA}^{r}$ at $m = N-1$. Thus each matrix in Eq. (D46) has compatible dimension $N-1\times N-1$. Substituting the fact that $\boldsymbol{C}_{4o} = \boldsymbol{A}_{12}\boldsymbol{C}_{\mathrm{IV}o}$ into Eq. (D46) produces

$$\boldsymbol{d} = \boldsymbol{C}_{\mathrm{IV}o}^{-1}\boldsymbol{A}_{12}^{-1}\boldsymbol{H}_{\boldsymbol{C}_{3o}}\boldsymbol{A}_{12}\boldsymbol{C}_{\mathrm{IV}o}\boldsymbol{\theta}, \tag{D47}$$

where the three interior matrices in Eq. (D47) commute, resulting in

$$\boldsymbol{d} = \boldsymbol{C}_{\mathrm{IV}o}^{-1}\boldsymbol{H}_{\boldsymbol{C}_{3o}}\boldsymbol{C}_{\mathrm{IV}o}\boldsymbol{\theta}, \tag{D48}$$

which is the desired result based on unitary transform matrices for Case 34.

**Case 35**

Case 35, $\boldsymbol{d} = \boldsymbol{S}_{4o}^{-1}\boldsymbol{H}_{\boldsymbol{C}_{4o}}\boldsymbol{S}_{3o}\boldsymbol{\theta}$, is not expressible in terms of unitary transform matrices because the matrix $\boldsymbol{A}_{16} = \boldsymbol{S}_{4o}\boldsymbol{S}_{\mathrm{IV}o}^{T}$ is not, in general, diagonal.

**Case 36**

Case 36, $\boldsymbol{d} = \boldsymbol{S}_{4o}^{-1}\boldsymbol{H}_{\boldsymbol{S}_{4o}}\boldsymbol{C}_{3o}\boldsymbol{\theta}$, is not expressible in terms of unitary transform matrices because the matrix $\boldsymbol{A}_{16} = \boldsymbol{S}_{4o}\boldsymbol{S}_{\text{IV}o}^{T}$ is not, in general, diagonal.

**Case 37**

Case 37, which states that

$$\boldsymbol{d} = -\boldsymbol{C}_{4o}^{-1}\boldsymbol{H}_{\boldsymbol{S}_{4o}}\boldsymbol{S}_{3o}\boldsymbol{\theta}, \tag{D49}$$

is expressible in terms of unitary transform matrices. The matrix $\boldsymbol{H}_{\boldsymbol{S}_{4o}} = \text{diag}\left\{\boldsymbol{S}_{4o}\boldsymbol{h}_{HAWS}^{r}\right\}$ normally contains $N$ samples ranging from 0 to $N-1$ along its diagonal, but here only the samples from 0 to $N-2$ need to be retained because the underlying symmetry of the vector $\boldsymbol{S}_{3o}\boldsymbol{\theta}$ forces a zero at $m = N-1$ which cancels the value of $\boldsymbol{S}_{4o}\boldsymbol{h}_{HAWS}^{r}$ at $m = N-1$. Thus each matrix in Eq. (D49) has compatible dimension $N-1 \times N-1$. Substituting the facts that $\boldsymbol{C}_{4o} = \boldsymbol{A}_{12}\boldsymbol{C}_{\text{IV}o}$ and $\boldsymbol{S}_{3o} = \boldsymbol{A}_{15}\boldsymbol{S}_{\text{III}o}$ into Eq. (D49) produces

$$\boldsymbol{d} = -\boldsymbol{C}_{\text{IV}o}^{-1}\boldsymbol{A}_{12}^{-1}\boldsymbol{H}_{\boldsymbol{S}_{4o}}\boldsymbol{A}_{15}\boldsymbol{S}_{\text{III}o}\boldsymbol{\theta}, \tag{D50}$$

where the three interior matrices in Eq. (D50) commute, resulting in

$$\boldsymbol{d} = -\boldsymbol{C}_{\text{IV}o}^{-1}\boldsymbol{H}_{\boldsymbol{S}_{4o}}\boldsymbol{S}_{\text{III}o}\boldsymbol{\theta}, \tag{D51}$$

because the matrices $\boldsymbol{A}_{12}$ and $\boldsymbol{A}_{15}$ are identical, and which is the desired result based on unitary transform matrices for Case 37.

**Case 38**

Case 38, $\boldsymbol{d} = \boldsymbol{C}_{3o}^{-1}\boldsymbol{H}_{\boldsymbol{C}_{4o}}\boldsymbol{C}_{4o}\boldsymbol{\theta}$, is not expressible in terms of unitary transform matrices because the matrix $\boldsymbol{A}_{11} = \boldsymbol{C}_{3o}\boldsymbol{C}_{\text{III}o}^{T}$ is not, in general, diagonal.

**Case 39**

Case 39, which states that

$$\boldsymbol{d} = \boldsymbol{S}_{3o}^{-1}\boldsymbol{H}_{\boldsymbol{S}_{4o}}\boldsymbol{C}_{4o}\boldsymbol{\theta}, \tag{D52}$$

is expressible in terms of unitary transform matrices. The matrix $\boldsymbol{H}_{\boldsymbol{S}_{4o}} = \text{diag}\{\boldsymbol{S}_{4o}\boldsymbol{h}_{HAWS}^{r}\}$ normally contains $N$ samples ranging from 0 to $N-1$ along its diagonal, but here only the samples from 0 to $N-2$ need to be retained because the underlying symmetry of the vector $\boldsymbol{C}_{4o}\boldsymbol{\theta}$ forces a zero at $m = N-1$ which cancels the value of $\boldsymbol{S}_{4o}\boldsymbol{h}_{HAWS}^{r}$ at $m = N-1$. Thus each matrix in Eq. (D52) has compatible dimension $N-1\times N-1$. Substituting the facts that $\boldsymbol{S}_{3o} = \boldsymbol{A}_{15}\boldsymbol{S}_{\text{III}o}$ and $\boldsymbol{C}_{4o} = \boldsymbol{A}_{12}\boldsymbol{C}_{\text{IV}o}$ into Eq. (D52) produces

$$\boldsymbol{d} = \boldsymbol{S}_{\text{III}o}^{-1}\boldsymbol{A}_{15}^{-1}\boldsymbol{H}_{\boldsymbol{S}_{4o}}\boldsymbol{A}_{12}\boldsymbol{C}_{\text{IV}o}\boldsymbol{\theta}, \tag{D53}$$

where the three interior matrices in Eq. (D53) commute, resulting in

$$\boldsymbol{d} = \boldsymbol{S}_{\text{III}o}^{-1}\boldsymbol{H}_{\boldsymbol{S}_{4o}}\boldsymbol{C}_{\text{IV}o}\boldsymbol{\theta}, \tag{D54}$$

because the matrices $\boldsymbol{A}_{12}$ and $\boldsymbol{A}_{15}$ are identical, and which is the desired result based on unitary transform matrices for Case 39.

**Case 40**

Case 40, $\boldsymbol{d} = -\boldsymbol{C}_{3o}^{-1}\boldsymbol{H}_{\boldsymbol{S}_{4o}}\boldsymbol{S}_{4o}\boldsymbol{\theta}$, is not expressible in terms of unitary transform matrices because the matrices $\boldsymbol{A}_{11} = \boldsymbol{C}_{3o}\boldsymbol{C}_{\text{III}o}^{T}$ and $\boldsymbol{A}_{16} = \boldsymbol{S}_{4o}\boldsymbol{S}_{\text{IV}o}^{T}$ are not, in general, diagonal.

## *Bibliography*


Ahmed, N., T. Natarajan, and K.R. Rao. "Discrete Cosine Transform." *IEEE Transactions on Computers* C-23, no. 1 (January 1974): 90–93.

Air Force Doctrine Document (AFDD) 1. *Air Force Basic Doctrine,* September 1997.

"Air Force Research Laboratory's Mission on Maui," *AMOS WWW Homepage,* 29 April 1998. On-line, Internet, Available from http://ulua.mhpcc.af.mil.

Ayers, G.R. and J.C. Dainty. "Iterative Blind Deconvolution Method and its Applications." *Optics Letters* 13, no. 7 (July 1988): 547–549.

Bongiovanni, Giancarlo, Paolo Corsini, and Graziano Frosini. "One Dimensional and Two-Dimensional Generalized Discrete Fourier Transforms." *IEEE Transactions on Acoustics, Speech, and Signal Processing* ASSP-24, no. 1 (February 1976): 97–99.

Davey, B.L.K., R.G. Lane, and R.H.T. Bates. "Blind Deconvolution of Noisy Complex-Valued Image." *Optics Communications* 69, no. 5,6 (January 15, 1989): 353–356.

Foltz, Thomas M. "Trigonometric Transforms for Image Reconstruction," Ph.D. Dissertation, AFIT/DS/ENG/98-04. Air Force Institute of Technology (AETC), Wright-Patterson AFB, Ohio, June 1998.

______ and B.M. Welsh. "Diagonal Forms of Symmetric Convolution Matrices for Asymmetric Multidimensional Sequences," in *Proceedings of the SPIE, Vol. 3460, Applications of Digital Image Processing XXI*, San Diego, Calif., (July 1998): 214–225.

______ and ______. "A Scalar Wiener Filter Based on Discrete Trigonometric Transforms and Symmetric Convolution," in *Proceedings of the SPIE, Vol. 3433, Propagation and Imaging through the Atmosphere II*, San Diego, Calif., (July 1998): 285–295.

______ and ______. "Image Reconstruction Using Symmetric Convolution and Discrete Trigonometric Transforms." *Journal of the Optical Society of America A* 15, no. 11 (November 1998): 2827–2840.

______ and ______. "Symmetric Convolution of Asymmetric Multidimensional Sequences Using Discrete Trigonometric Transforms," to appear in *IEEE Transactions on Image Processing* 8, no. 5 (May 1999).

______, ______, and C.D. Holmberg. "Symmetric Convolution Using Unitary Transform Matrices," submitted to *IEEE Transactions on Signal Processing.*

Ford, Stephen D. "Linear Reconstruction of Non-Stationary Image Ensembles Incorporating Blur and Noise Models," Ph.D. Dissertation, AFIT/DS/ENG/98-02. Air Force Institute of Technology (AETC), Wright-Patterson AFB, Ohio, March 1998.

Gonzalez, Rafael C. and Richard E. Woods. *Digital Image Processing*. Reading, Mass.: Addison-Wesley, 1992.

Goodman, Joseph W. *Fourier Optics*. New York: McGraw-Hill, 1968.

______. *Statistical Optics*. New York: John Wiley and Sons, 1985.

Hardy, John W. "Adaptive Optics—Technology developed during the cold war is giving new capabilities to ground-based astronomical telescopes." *Scientific American* 270, no. 6 (June 1994): 60–65.

Helstrom, Carl W. "Image Restoration by the Method of Least Squares." *Journal of the Optical Society of America* 57, no. 3 (March 1967): 297–303.

Hunt, B.R. "A Matrix Theory Proof of the Discrete Convolution Theorem." *IEEE Transactions on Audio and Electroacoustics* AU-19, no. 4 (December 1971): 285–288.

______. "The Application of Constrained Least Squares Estimation to Image Restoration by Digital Computer." *IEEE Transactions on Computers* C-22, no. 9 (September 1973): 805–812.

Jain, Anil K. "A Sinusoidal Family of Unitary Transforms." *IEEE Transactions on Pattern Analysis and Machine Intelligence* PAMI-1, no. 4 (October 1979): 356–365.

______. *Fundamentals of Digital Image Processing*. Englewood Cliffs, N.J.: Prentice-Hall, 1989.

Kay, Steven M. *Fundamentals of Statistical Signal Processing*. Englewood Cliffs, N.J.: Prentice-Hall, 1993.

Kekre, H.B. and J.K. Solanki. "Comparative Performance of Various Trigonometric Unitary Transforms for Image Coding." *International Journal of Electronics* 44, no. 3 (March 1978): 305–315.

Martucci, Stephen A. "Symmetric Convolution and the Discrete Sine and Cosine Transforms." *IEEE Transactions on Signal Processing* 42, no. 5 (May 1994): 1038–1051.

______. "Image Resizing in the Discrete Cosine Transform Domain," in *Proceedings of the IEEE International Conference on Image Processing*, vol. 2, Washington, D.C., (October 1995): 244–247.

______. "Digital Filtering of Images Using the Discrete Sine and Cosine Transforms." *Optical Engineering* 35, no. 1 (January 1996): 119–127.

*National Military Strategy of the United States of America*, September 1997.

Oppenheim, Alan V. and Ronald W. Schafer. *Digital Signal Processing*. Englewood Cliffs, N.J.: Prentice-Hall, 1975.

Pratt, William K. "Generalized Wiener Filter Computation Techniques." *IEEE Transactions on Computers* C-21, no. 7 (July 1972): 636–641.

______. *Digital Image Processing*. New York: John Wiley and Sons, 1978.

Rao, K.R. and P. Yip. *Discrete Cosine Transform: Algorithms, Advantages, Applications*. San Diego: Academic Press, 1990.

Roggemann, Michael C. and Byron M. Welsh. *Imaging Through Turbulence*. Boca Raton, Fla.: CRC Press, 1996.

Sánchez, Victoria, Pedro García, Antonio M. Peinado, José C. Segura, and Antonio J. Rubio. "Diagonalizing Properties of the Discrete Cosine Transforms." *IEEE Transactions on Signal Processing* 43, no. 11 (November 1995): 2631–2641.

Sánchez, Victoria, Antonio M. Peinado, José C. Segura, Pedro García, and Antonio J. Rubio, "Generating Matrices for the Discrete Sine Transforms." *IEEE Transactions on Signal Processing* 44, no. 10 (October 1996): 2644–2646.

Scharf, Loius L. *Statistical Signal Processing: Detection, Estimation, and Time Series Analysis*. Reading, Mass.: Addison-Wesley, 1991.

Slepian, David. “Linear Least-Squares Filtering of Distorted Images.” *Journal of the Optical Society of America* 57, no. 7 (July 1967): 918–922.

Standley, Clive. “Adaptive Optics Compensates for Atmospheric Distortion.” *Laser Focus World* 34, no. 6 (June 1998): 90–95.

Therrien, Charles W. *Discrete Random Signals and Statistical Signal Processing*. Englewood Cliffs, N.J.: Prentice-Hall, 1992.

Thompson, Laird A. “Adaptive Optics in Astronomy.” *Physics Today* 47, no. 12 (December 1994): 24–31.

Wang, Zhongde. “Fast Algorithms for the Discrete W Transform and for the Discrete Fourier Transform.” *IEEE Transactions on Acoustics, Speech, and Signal Processing* ASSP-32, no. 4 (August 1984): 803–816.

______ and B.R. Hunt. “The Discrete W Transform.” *Applied Mathematics and Computation* 16, no. 1 (January 1985): 19–48.

Wiener, Norbert. *Extrapolation, Interpolation, and Smoothing of Stationary Time Series*. New York: John Wiley and Sons, 1949.